A Generalized Knockoff Procedure for FDR Control in Structural Change Detection

Jingyuan Liu^a, Ao Sun^a and Yuan Ke^b

^aMOE Key Laboratory of Econometrics, Department of Statistics,
School of Economics, Wang Yanan Institute for Studies in Economics
and Fujian Key Lab of Statistics, Xiamen University, P.R China

^bDepartment of Statistics, University of Georgia, Athens, GA 30602, USA

Abstract. Controlling false discovery rate (FDR) is crucial for variable selection, multiple testing, among other signal detection problems. In literature, there is certainly no shortage of FDR control strategies when selecting individual features. Yet lack of relevant work has been done regarding structural change detection, including, but not limited to change point identification, profile analysis for piecewise constant coefficients, and integration analysis with multiple data sources. In this paper, we propose a generalized knockoff procedure (GKnockoff) for FDR control under such problem settings. We prove that the GKnockoff possesses pairwise exchangeability, and is capable of controlling the exact FDR under finite sample sizes. We further explore GKnockoff under high dimensionality, by first introducing a new screening method to filter the highdimensional potential structural changes. We adopt a data splitting technique to first reduce the dimensionality via screening and then conduct GKnockoff on the refined selection set. Numerical comparisons with other methods show the superior performance of GKnockoff, in terms of both FDR control and power. We also implement the proposed method to analyze a macroeconomic dataset for detecting change points in the consumer price index, as well as the unemployment rate.

Keywords. Structural change detection; False discovery rate control; Knockoffs; High dimensional data; Screening

1 Introduction

The era of information explosion has driven researchers from squeezing limited data to extracting useful messages from massive amounts of data. Plentiful works have been developed for detecting important features, ranging from regularized regression (Tibshirani, 1996; Fan and Li, 2001; Zhang, 2010; Fan et al., 2020) to screening-related approaches (Fan and Lv, 2008; Li et al., 2012; Liu et al., 2014; Mai and Zou, 2015; Ma et al., 2017; Liu et al., 2021). See Fan and Lv (2018), Liu et al. (2015) and Fan et al. (2020) for summaries of important works among those lines. Meanwhile, apart from identifying individual features, structural change detection is also of great scientific interest, especially in the realm of finance, genomics, health care, social science, and so forth. For instance, identifying the impact of economic structural changes, such as those of consumer price index (CPI) and unemployment rate analyzed in Section 5, is a crucial task in the macroeconomic study since the structural changes might alter economic assumptions for determining courses of action (Ramey, 2016). The structural changes non-exhaustively include jump points in time series, effect changes in piecewise constant coefficient models, and heterogenous coefficients upon integrating multiple data sources. Harchaoui and Lévy-Leduc (2007) detected locations of change points in one-dimensional piecewise constant signals. Zou et al. (2014) proposed a nonparametric maximum likelihood approach for multiple change-point problems. Cho and Fryzlewicz (2015) proposed a sparsified binary segmentation method to detect multiple change points in high-dimensional time series. Niu et al. (2016) discussed a normal mean multiple change-point model (MCM) from the perspectives of estimation, consistency and inference. Wang et al. (2018) considered the change-point detection in multinomial data with a large number of categories. As to integration of multiple data sources, Ke et al. (2015) proposed a CARDS method to first order the coefficients and then fuse the adjacent coefficients. Chen and Zhang (2015) studied a graph-based change point detection method. Wang et al. (2016) applied the CARDS idea to combine multiple studies with repeated measurements to reduce the coefficients constraints and gain computational efficiency. Tang and Song (2016) utilized fused Lasso (Tibshirani et al., 2005) to identify the heterogenous coefficients by merging inter-study homogeneous parameter clusters. More recent developments include Avanesov and Buzun (2018), Wang et al. (2020), Jiang et al. (2020), Dette et al. (2020), Xiao et al. (2021), among many others.

Admittedly, researchers have devoted much attention to detecting structural changes. Another

crucial question to consider, however, is how "scientific" the discoveries are - if the extracted information consists of too many falsely discovered signals that are merely selected to fit the current random sample, we would be stuck in the "reproducible crisis" that deeply undermines the reliability of statistical findings. The false discoveries are attributed in part to the classical error accumulation issue raised by multiple testing, and the spurious correlations (Fan and Lv, 2008; Fan et al., 2012). The spurious correlation between a certain feature and the response refers to the respective association that is exhibited merely by the current specific sample, rather than the nature of the population relationship. For instance, a spurious feature might seem to be predictive to the response because it is correlated with some true predictors. Unfortunately, such spuriousness can not be revealed by standard signal detection techniques. For feature selection problem, Su et al. (2017) demonstrated that the true and null features often intersperse on the Lasso solution path when all features are independently generated from an identical Gaussian distribution, and this phenomenon occurs under whatsoever effect sizes. Then directly selecting nonzero coefficients along the solution path fails to control false discoveries. For change-point detection, Rojas and Wahlberg (2014) showed that fused Lasso in the normal mean MCM model tends to identify the spurious points, and the falsely selected points will not disappear asymptotically.

Accordingly, there is an eager appeal of controlling the degree of false discoveries, typically measured by the false discovery rate (FDR), to enhance the reliability of structural change detection. The concept of FDR was first advocated by Benjamini and Hochberg (1995), calculated as the expected proportion of false discoveries among all discoveries. To be specific, let \mathcal{S} be the index set of the true signals, and $\hat{\mathcal{S}}$ be that of the discovered signals based on the sampled data. The FDR is defined as

$$FDR = E\left[\frac{|\hat{S} \setminus S|}{|\hat{S}|}\right]. \tag{1.1}$$

For independent multiple testing problems, Benjamini and Hochberg (1995) developed a sequential Bonferroni-type method, called the B-H procedure, to control FDR based on the ordered individual p-values. Benjamini and Yekutieli (2001) showed that the B-H procedure also works under the assumption of "positive regression dependence on a subset". They further advocated a B-Y method by adding a divisor to the threshold of B-H, and proved that B-Y can control FDR under arbitrary dependence structures. Refer to Benjamini (2010) for a comprehensive overview

of the B-H-type methods. A more recent milestone of FDR control is the proposal of knockoff filter (Barber and Candès, 2015). It constructs "knockoffs" for the original features that mimic the correlation structure among features yet are known to be independent of the response. Then the knockoffs might serve as references for estimating and hence controlling FDR by regressing the response on both original and knockoff features. Under mild conditions, the knockoff filter achieves exact FDR control in finite sample settings. Weinstein et al. (2017) proved that the knockoff filter from an independent and identically distributed Gaussian design asymptotically achieves optimal power. Dai and Barber (2016) extended the knockoff filter to grouped feature selection. Candès et al. (2018) developed a model-X knockoff procedure that can be applied to the high-dimensional regime, provided the prior knowledge about the joint distributions of the original features. Fan et al. (2018) constructed the model-X knockoffs when the covariates follow a Gaussian graphical model. Lu et al. (2018) integrated the model-X knockoff framework with the deep neural networks (DNN) architecture to enhance the interpretability and reproducibility of DNN. If the joint distribution of features is unknown, Fan et al. (2020) and Romano et al. (2020) constructed the knockoff variables by imposing a latent factor model and a deep generative model, respectively.

Notwithstanding the merit of knockoffs, few related literature, to our best knowledge, is amenable to the structural change detection. Thus in this paper, we propose a unified approach, called generalized knockoff (GKnockoff), that rigorously controls FDR for structural change problems under finite sample sizes. Consider the classical linear regression model

$$\mathbf{y} = \mathbf{X}\boldsymbol{\beta} + \boldsymbol{\epsilon},\tag{1.2}$$

where $\mathbf{y} \in \mathbb{R}^n$ is a sample vector of response, $\mathbf{X} \in \mathbb{R}^{n \times p}$ is a design matrix, $\boldsymbol{\beta} = (\beta_1, \dots, \beta_p)^{\top} \in \mathbb{R}^p$ is an unknown vector of coefficients, and $\boldsymbol{\epsilon}$ is independent with \mathbf{X} . Further, we assume the elements in $\boldsymbol{\epsilon}$ are i.i.d. normal random errors with mean 0 and variance σ^2 . While variable selection identifies nonzero β_j 's, structural change detection typically concerns about the linear combinations, $\mathbf{d}_j^{\top} \boldsymbol{\beta}$, $j = 1, \dots, m$, for some properly defined $\mathbf{d}_j \in \mathbb{R}^p$, where m is the number of linear combinations under consideration. Take piecewise constant coefficients profile for instance, it is of interest to detect $\{j = 1, \dots, p-1 : \beta_{j+1} - \beta_j \neq 0\}$; namely, m = p-1, and $\mathbf{d}_j = (0, \dots, 0, -1, 1, 0, \dots, 0)^{\top}$, whose (j+1)th element is 1 and jth element is -1. In addition, variable selection could as well

belong to this structural change category by defining $\mathbf{d}_j = (0, \dots, 0, 1, 0, \dots, 0)^{\top}$ with 1 appearing in the jth position. More examples of structural change are discussed in Section 2. Therefore, the objective is indeed to identify the active set $\mathcal{S} = \{j = 1, \dots, m : \mathbf{d}_j^{\top} \boldsymbol{\beta} \neq 0\}$ while controlling FDR.

The main obstacle of constructing knockoffs for such problems is twofold. Firstly, we apply a fullrow-rank transformation matrix to transform the original samples, and then recover the active set \mathcal{S} by a partial regularization method. However, the transformed samples are no longer independent and hence violate the assumption for the theories in Barber and Candès (2015). To tackle this challenge, we propose a generalized knockoff procedure, named GKnockoff, for the transformed data. We show that the GKnockoff variables enjoy the exchangeability without the independence assumption, and prove that GKnockoff can rigorously control FDR. Secondly, The framework of Barber and Candès (2015) does not apply to the high-dimensional regime, as the construction of knockoff features requires the sample size to be at least twice the number of features. As a primitive philosophy of quickly reducing dimensionality, screening has been extensively studied over the past decade since the pioneering work of Fan and Lv (2008). However, compared with ubiquitous techniques for screening individual features based on various models, our understanding of how to screen structural changes seems limited, so to speak. For normal mean MCM, Niu and Zhang (2012) proposed a screening and ranking algorithm and showed the sure coverage property, which means the true change points belong to the neighborhood of the points in the selection set with an overwhelming probability. Ke et al. (2014) proposed a covariate-assisted approach to enhance the selection power in finite samples. The general structural change screening, however, was seldom tackled in literature. The challenge is in part attributed to that screening individual features is a matter of teasing apart signals from noise, thus it only requires effects of active features to be non-vanishingly estimated, typically large. Meanwhile, screening structural changes, e.g. coefficient changes, which aims to discover the "difference in coefficients", calls for the ability to accurately quantify the amplitude of individual coefficients. Accordingly, we develop a new screening procedure for structural change detection and study its theoretical and empirical performances. Also, we adopt a data splitting technique (e.g. Wasserman and Roeder, 2009; Barber and Candès, 2019; Liu et al., 2021) to alternatively filtering structural changes and constructing GKnockoffs on two halves of data. Furthermore, we develop an efficient and user-friendly R package 'GKnockoff' to implement the GKnockoff procedure.

1.1 Notations

We introduce the following notations used throughout this paper. Denote \mathbb{R} the set of real numbers. For a set \mathcal{A} , $|\mathcal{A}|$ denotes its cardinality. Given a vector $\mathbf{x} = [x_1, \ldots, x_d]^{\top} \in \mathbb{R}^d$, we write the vector l_q -norm as $\|\mathbf{x}\|_q := \left(\sum_{j=1}^d |x_j|^q\right)^{1/q}$ for $1 \leq q < \infty$ and the vector l_{∞} -norm as $\|\mathbf{x}\|_{\infty} := \max_{1 \leq j \leq d} |x_j|$. Denote diag $\{\mathbf{x}\}$ a diagonal matrix whose diagonal elements belong to \mathbf{x} . For a matrix $\mathbf{A} = [\mathbf{A}_{(k,l)}]_{1 \leq k \leq d_1; 1 \leq l \leq d_2} \in \mathbb{R}^{d_1 \times d_2}$, the ∞ -norm of \mathbf{A} is denoted as $|||\mathbf{A}|||_{\infty} := \max_k \sum_{l=1}^{d_2} |\mathbf{A}_{(k,l)}|$. The jth column of \mathbf{A} is denoted A_j , and $A_{\mathcal{G}}$ refers to the columns of \mathbf{A} with indexes in the set \mathcal{G} . If \mathbf{A} is a symmetric matrix, $\lambda_{\max}(\mathbf{A})$ and $\lambda_{\min}(\mathbf{A})$ are respectively its largest and smallest eigenvalues. We write $\mathbf{A} \succeq 0$ if \mathbf{A} is a positive semi-definite matrix. $\mathbf{0}_d$, $\mathbf{0}_{d \times d}$ and \mathbf{I}_d denote the d-dimensional vector of zeros, the $d \times d$ -dimensional matrix of zeros, and the d-dimensional identity matrix, respectively. For $a,b \in \mathbb{R}$, we denote sign(a) the sign function of a, and $a \vee b$ the maximum between a and b. When necessary, we consider 0/0 = 0. For two matrices \mathbf{A} and \mathbf{B} of the same dimension, the operator $[\mathbf{A}, \mathbf{B}]_{\text{swap}(\mathcal{G})}$ refers to swapping the jth column in \mathbf{A} and the jth column in \mathbf{B} for all $j \in \mathcal{G}$.

1.2 Organization of the paper

The rest of the paper is organized as follows. In Section 2, we propose a generalized knockoff (GKnockoff) framework to detect structural changes and control FDR. We define a GKnockoff matrix and discuss the intuition and the implementation of a GKnockoff filter. We also provide the theoretical guarantees of GKnockoff for controlling FDR under finite samples. Section 3 is devoted to the high-dimensional structural change detection and FDR control problem, where we introduce a screening technique named FuSIS and a high-dimensional GKnockoff filter. The superior performance of GKnockoff is empirically verified through several simulation studies in Section 4. In Section 5, we apply the proposed method to study a macroeconomic dataset and detect structural changes in CPI and the unemployment rate. Section 6 concludes the paper. The

¹https://github.com/suntiansheng/Gknockoff

proofs of theoretical results and some useful technical lemmas are presented in the Appendix.

2 A generalized knockoff framework

2.1 Problem setup

As we discussed in the introduction, many structural change detection problems can be formulated by the linear model (1.2) and the m hypotheses as follows.

$$H_{0j}: \mathbf{d}_i^{\mathsf{T}} \boldsymbol{\beta} = 0 \quad \text{v.s.} \quad H_{1j}: \mathbf{d}_i^{\mathsf{T}} \boldsymbol{\beta} \neq 0, \quad j = 1, \dots, m,$$

where $\mathbf{d}_j \in \mathbb{R}^p$ is a problem-driven transformation vector. Further, we denote $\mathcal{S} = \{j = 1, ..., m : \mathbf{d}_j^\top \boldsymbol{\beta} \neq 0\}$ the active set of the structural change detection problem, and $\mathcal{S}^c = \{1, ..., m\} \setminus \mathcal{S}$ the inactive set. Let $\mathbf{D} = [\mathbf{d}_1, ..., \mathbf{d}_m]^\top \in \mathbb{R}^{m \times p}$. We then estimate the regression coefficients and recover the active set \mathcal{S} simultaneously by solving a generalized Lasso problem (Tibshirani and Taylor, 2011)

$$\min_{\mathbf{b} \in \mathbb{R}^p} \frac{1}{2n} \|\mathbf{y} - \mathbf{X}\mathbf{b}\|_2^2 + \lambda \|\mathbf{D}\mathbf{b}\|_1, \tag{2.1}$$

where $\lambda \geq 0$ is a regularization parameter. The model setup (2.1) is applicable to a wide range of structural change detection problems. Next, we discuss the design of the transformation matrix **D** in three popular scenarios.

Scenario 1: Multiple change points detection

Let $\mathbf{y} = [y_1, \dots, y_n]^{\top}$ be a sequence of random variables with $y_i = \mu_i + \epsilon_i$, i = 1, ..., n, where ϵ_i 's are i.i.d. $N(0, \sigma^2)$. Suppose $\boldsymbol{\mu} = [\mu_1, ..., \mu_n]^{\top}$ is a piecewise constant vector, such that $\mu_1 = \ldots = \mu_{\tau_1} \neq \mu_{\tau_1+1} = \ldots = \mu_{\tau_2} \neq \mu_{\tau_2+1} = \ldots = \mu_{\tau_J} \neq \mu_{\tau_J+1} = \ldots = \mu_n$. Let $\mathcal{S} = \{\tau_1, \dots, \tau_J\}$ be the set of all jump locations. This model is called normal mean multiple change-point model (normal mean MCM, see Niu et al., 2016). To recover \mathcal{S} by (2.1), we set p = n, $\mathbf{X} = \mathbf{I}_n$, and $\boldsymbol{\beta} = \boldsymbol{\mu}$. Then,

we choose m = n - 1 and design the transformation matrix **D** as

$$\mathbf{D} = \begin{bmatrix} -1 & 1 & 0 & \cdots & 0 & 0 \\ 0 & -1 & 1 & \cdots & 0 & 0 \\ \vdots & \vdots & \vdots & \vdots & \vdots & \vdots \\ 0 & 0 & 0 & \cdots & -1 & 1 \end{bmatrix}_{m \times n} . \tag{2.2}$$

Scenario 2: Piecewise constant coefficients profile

Piecewise constant coefficients profile (or homogeneity pursuit, see Ke et al., 2015) is an extension of normal mean MCM for the linear regression model (1.2) with a general $n \times p$ design matrix \mathbf{X} . To be specific, we assume the p coefficients β_1, \ldots, β_p can be segmented into J+1 groups, such that $\beta_1 = \ldots = \beta_{\tau_1} \neq \beta_{\tau_1+1} = \ldots = \beta_{\tau_2} \neq \beta_{\tau_2+1} = \ldots = \beta_{\tau_J} \neq \beta_{\tau_J+1} = \ldots = \beta_p$. Let $\mathcal{S} = \{\tau_1, \ldots, \tau_J\}$ be the set of all change locations. To recover \mathcal{S} by (2.1), we can choose set m = p - 1 and design \mathbf{D} in the format as (2.2).

Scenario 3: Integration analysis from multiple data sources

Due to the rapid development of data collecting techniques, it has been attractive yet challenging to integrate high-throughput data from multiple sources into a unified regression framework. Suppose there are K available data sources. For the kth data source, $k = 1, \ldots, K$, we observe a random sample $(\mathbf{y}^{(k)}, \mathbf{X}^{(k)})$ and fit a linear regression model $\mathbf{y}^{(k)} = \mathbf{X}^{(k)}\boldsymbol{\beta}^{(k)} + \boldsymbol{\epsilon}^{(k)}$, where $\mathbf{X}^{(k)} \in \mathbb{R}^{n_k \times p}$ and $\boldsymbol{\epsilon}^{(k)} \sim N(0, \sigma^2 \mathbf{I}_{n_k})$. It is natural to test weather there is a homogeneous structure embedded among the coefficient vectors $\{\boldsymbol{\beta}^{(1)}, \ldots, \boldsymbol{\beta}^{(K)}\}$. To that end, we can formulate (2.1) as

$$\min_{\boldsymbol{\beta} \in \mathbb{R}^{K \times p}} \frac{1}{2n} \begin{bmatrix} \mathbf{y}^{(1)} \\ \mathbf{y}^{(2)} \\ \vdots \\ \mathbf{y}^{(K)} \end{bmatrix} - \begin{bmatrix} \mathbf{X}^{(1)} & \dots & \mathbf{0} \\ \vdots & \ddots & \vdots \\ \mathbf{0} & \dots & \mathbf{X}^{(K)} \end{bmatrix} \begin{bmatrix} \mathbf{b}^{(1)} \\ \mathbf{b}^{(2)} \\ \vdots \\ \mathbf{b}^{(K)} \end{bmatrix} \begin{vmatrix} 2 \\ + \lambda \\ \mathbf{D} \begin{bmatrix} \mathbf{b}^{(1)} \\ \mathbf{b}^{(2)} \\ \vdots \\ \mathbf{b}^{(K)} \end{bmatrix} \end{vmatrix}, \qquad (2.3)$$

where the transformation matrix \mathbf{D} can be designed as

$$\mathbf{D} = \begin{bmatrix} \mathbf{I}_{p} & -\mathbf{I}_{p} & \mathbf{0}_{p \times p} & \dots & \mathbf{0}_{p \times p} & \mathbf{0}_{p \times p} \\ \mathbf{0}_{p \times p} & \mathbf{I}_{p} & -\mathbf{I}_{p} & \dots & \mathbf{0}_{p \times p} & \mathbf{0}_{p \times p} \\ \vdots & \vdots & \vdots & \vdots & \vdots & \vdots \\ \mathbf{0}_{p \times p} & \mathbf{0}_{p \times p} & \mathbf{0}_{p \times p} & \dots & \mathbf{I}_{p} & -\mathbf{I}_{p} \end{bmatrix}_{(K-1)p \times Kp}$$
(2.4)

Beyond the above examples, the regularization regression (2.1) and the transformation matrix **D** can be tailored for a wide range of structural change detection problems. Further, our problem setup has the penitential to be applied to other high-dimensional testing problems where the hypothesis can be characterized by a linear combination of regression coefficients. See Li and Li (2021) as a recent study in this direction, among others.

2.2 Structural change detection

In this subsection, we study the detection of structural changes by solving the generalized Lasso problem (2.1). Suppose \mathbf{D} is of full row rank. We first define $\tilde{\mathbf{D}} = [\mathbf{D}^{\top}, \mathbf{E}^{\top}]^{\top} \in \mathbb{R}^{p \times p}$ such that $\tilde{\mathbf{D}}$ has full rank, with \mathbf{E} being any matrix in the complementary space of the linear space spanned by \mathbf{D} . We also define $\boldsymbol{\theta} = (\boldsymbol{\theta}_1^{\top}, \boldsymbol{\theta}_2^{\top})^{\top} = \tilde{\mathbf{D}}\boldsymbol{\beta}$, where $\boldsymbol{\theta}_1 = [\theta_{11}, \dots, \theta_{1m}]^{\top} = \mathbf{D}\boldsymbol{\beta}$ and $\boldsymbol{\theta}_2 = \mathbf{E}\boldsymbol{\beta}$. Then, the non-zero elements in $\boldsymbol{\theta}_1$ reflect the structural changes of interest and the active set can be represented as $\mathcal{S} = \{j = 1, \dots, m : \theta_{1j} \neq 0\}$. Further, denote the inverse matrix of $\tilde{\mathbf{D}}$ as $\tilde{\mathbf{D}}^{-1} = [\mathbf{Z}_{p \times m}, \mathbf{F}_{p \times (p-m)}]$, where $\mathbf{Z}_{p \times m}$ and $\mathbf{F}_{p \times (p-m)}$ stand for the first m and the rest (p-m) columns of $\tilde{\mathbf{D}}^{-1}$ respectively. Therefore, we have $\boldsymbol{\beta} = \tilde{\mathbf{D}}^{-1}\boldsymbol{\theta} = \mathbf{Z}\boldsymbol{\theta}_1 + \mathbf{F}\boldsymbol{\theta}_2$. With the above preparations, we can reformulate (2.1) as a partial regularization problem

$$\min_{\boldsymbol{\theta} = [\boldsymbol{\theta}_1^{\mathsf{T}}, \boldsymbol{\theta}_2^{\mathsf{T}}]^{\mathsf{T}} \in \mathbb{R}^p} \frac{1}{2n} \|\mathbf{y} - \mathbf{X}\mathbf{Z}\boldsymbol{\theta}_1 - \mathbf{X}\mathbf{F}\boldsymbol{\theta}_2\|_2^2 + \lambda \|\boldsymbol{\theta}_1\|_1,$$
(2.5)

where $\lambda \geq 0$ is a regularization parameter. Notice that, when **D** is designed as in (2.2), the formulation in (2.5) becomes a fused Lasso problem (Tibshirani et al., 2005).

We then adopt the partial residual technique (e.g. Hsiao et al., 2021; Zou and Li, 2008) and

transfer (2.5) to a Lasso-type problem

$$\min_{\boldsymbol{\theta}_1 \in \mathbb{R}^m} \frac{1}{2n} \|\mathbf{y}^* - \mathbf{X}^* \boldsymbol{\theta}_1\|_2^2 + \lambda \|\boldsymbol{\theta}_1\|_1, \tag{2.6}$$

where $\mathbf{y}^* = \mathbf{M}\mathbf{y}$, $\mathbf{X}^* = \mathbf{M}\mathbf{X}\mathbf{Z}$, and $\mathbf{M} := \mathbf{I}_n - (\mathbf{X}\mathbf{F})[(\mathbf{X}\mathbf{F})^{\top}(\mathbf{X}\mathbf{F})]^{-1}(\mathbf{X}\mathbf{F})^{\top}$ is a projection matrix. The transformed design matrix \mathbf{X}^* consists of m columns, each of which is associated with a potential structural change. A key observation from (2.6) is that the elements in \mathbf{y}^* are no longer independent since

$$\mathbf{y}^* = \mathbf{M}\mathbf{y} \sim N(\mathbf{X}^*\boldsymbol{\theta}_1, \sigma^2 \mathbf{M}). \tag{2.7}$$

Such dependence violates the independence assumption imposed for the theoretical analysis of knockoff filter (Barber and Candès, 2015), and hence calls new methodological and theoretical investigations. In the rest of this subsection, we derive the selection consistency and asymptotic power for the solution of (2.6). In the next subsection, we introduce a generalized knockoff filter to control FDR under the dependence structure.

We establish selection consistency using the Primal-Dual Witness technique (Wainwright, 2009). Without loss of generality, we assume that X_j^* is normalized such that $n^{-1/2} \max_j ||X_j^*|| \leq 1$, $j = 1, \ldots, m$, to simplify the presentation in the theoretical analysis. In addition, we impose the following two conditions to pave the way for the selection consistency results presented in Theorem 2.1 below.

Condition 2.1. $|||\mathbf{X}_{S^c}^{*\top}\mathbf{X}_{S}^{*}(\mathbf{X}_{S}^{*\top}\mathbf{X}_{S}^{*})^{-1}|||_{\infty} \leq 1 - \kappa \text{ for some constant } \kappa \in (0,1].$

Condition 2.2. $\Lambda_{\min}(\mathbf{X}_{\mathcal{S}}^{*\top}\mathbf{X}_{\mathcal{S}}^{*}/n) \geq C_{\min} \text{ for some constant } C_{\min} > 0,$

Condition 2.1, which requires the active and inactive variables not to be too correlated, is a common technique condition considered in previous work of Lasso, see, for example, Zhao and Yu (2006) and Wainwright (2009). Condition 2.2 states the minimum eigenvalue of Gram matrix of the true set is bounded away from zero and thus the Gram matrix is invertible.

Theorem 2.1. Under Conditions 2.1 and 2.2, suppose $\lambda > \frac{2}{\kappa} \sqrt{\frac{2\sigma^2 \log p}{n}}$ in (2.6), then for some $c_1 > 0$, the following properties hold with probability greater than $1 - 4 \exp(-c_1 n \lambda^2)$.

(a) The generalized Lasso has a unique solution $\hat{\boldsymbol{\theta}}_1$ with $\mathcal{S} \subset \hat{\mathcal{S}}$, where $\hat{\mathcal{S}} = \{j = 1, \dots, m: \hat{\theta}_{1j} \neq 1\}$

0}. And the estimate $\hat{\boldsymbol{\theta}}_{1S}$ of the truly non-vanishing coefficient $\boldsymbol{\theta}_{1S}$ satisfies

$$||\hat{\boldsymbol{\theta}}_{1S} - \boldsymbol{\theta}_{1S}||_{\infty} \le g(\lambda), \tag{2.8}$$

where
$$g(\lambda) = \lambda \left[|||(\mathbf{X}_{\mathcal{S}}^{*\top} \mathbf{X}_{\mathcal{S}}^{*}/n)^{-1}|||_{\infty} + \frac{4\sigma}{\sqrt{C_{\min}}} \right].$$

(b) If we further assume $\min(|\boldsymbol{\theta}_{1S}|) \geq g(\lambda)$, then the generalized Lasso estimator has the correct sign, i.e. $\operatorname{sign}(\hat{\boldsymbol{\theta}}_1) = \operatorname{sign}(\boldsymbol{\theta}_1)$.

Theorem 2.1 (a) guarantees that the generalized Lasso under the dependence structure enjoys the sure screening property (Fan and Lv, 2008), and hence a full asymptotic power; and the estimation errors are uniformly bounded above. Theorem 2.1 (b) further implies the selection consistency, thus the asymptotic FDR is zero. Nevertheless, the finite sample FDR control, as to be discussed in the next section, is of more interest for practitioners.

2.3 Generalized knockoff filter and FDR control

In this subsection, we introduce a generalized knockoff (GKnockoff) filter and an FDR control procedure. Denote $\Sigma^* = \mathbf{X}^{*\top}\mathbf{X}^* = \mathbf{Z}^{\top}\mathbf{X}^{\top}\mathbf{M}\mathbf{X}\mathbf{Z}$ the Gram matrix of \mathbf{X}^* . The $n \times m$ matrix of GKnockoff features $\tilde{\mathbf{X}}$ should satisfy

$$\tilde{\mathbf{X}}^{\top}\tilde{\mathbf{X}} = \mathbf{\Sigma}^*, \text{ and } \tilde{\mathbf{X}}^{\top}\mathbf{X}^* = \mathbf{\Sigma}^* - \operatorname{diag}\{\mathbf{s}\} \succeq 0.$$
 (2.9)

The matrix $\tilde{\mathbf{X}}$ can be considered as a second-order knockoff copy of \mathbf{X}^* for the following reasons. First, given \mathbf{X}^* , $\tilde{\mathbf{X}}$ is independent of \mathbf{y}^* since we do not use the information of \mathbf{y}^* in (2.9). Second, the Gram matrix remains after column-wise swapping, i.e., $[\mathbf{X}^*, \tilde{\mathbf{X}}]_{\text{swap}(\mathcal{G})}^{\top}[\mathbf{X}^*, \tilde{\mathbf{X}}]_{\text{swap}(\mathcal{G})}^{\top} = [\mathbf{X}^*, \tilde{\mathbf{X}}]^{\top}[\mathbf{X}^*, \tilde{\mathbf{X}}]$ for any $\mathcal{G} \subset \{1, 2, ..., m\}$. When $n \geq 2m$, one can compute $\tilde{\mathbf{X}}$ by

$$\tilde{\mathbf{X}} = \mathbf{X}^* \left(\mathbf{I}_m - \mathbf{\Sigma}^{*-1} \operatorname{diag}\{\mathbf{s}\} \right) + \tilde{\mathbf{U}}\mathbf{C}$$
(2.10)

for some $\mathbf{s} = (s_1, \dots, s_m)^{\top} \in \mathbb{R}_+^m$ satisfying $2\mathbf{\Sigma}^* - \operatorname{diag}(\mathbf{s}) \succeq 0$. Moreover, $\tilde{\mathbf{U}}$ is in the null space of \mathbf{X}^* , i.e. $\mathbf{X}^{*\top}\tilde{\mathbf{U}} = 0$ and \mathbf{C} is the Cholesky decomposition of $2\operatorname{diag}\{\mathbf{s}\} - \operatorname{diag}\{\mathbf{s}\}\mathbf{\Sigma}^{*-1}\operatorname{diag}\{\mathbf{s}\}$.

The following theorem presents one of our main findings, that \mathbf{X}^* and its GKnockoff copy $\tilde{\mathbf{X}}$

possess the pairwise exchangeability, which is crucial to the function of GKnockoff, yet not trivial since the elements in \mathbf{y}^* are no longer independent.

Theorem 2.2 (pairwise exchangeability). Let $\mathcal{G} \subset \mathcal{S}^c$. Then, we have

$$[\mathbf{X}^*, \tilde{\mathbf{X}}]_{\mathrm{swap}(\mathcal{G})}^{\top} \mathbf{y}^* \stackrel{d}{=} [\mathbf{X}^*, \tilde{\mathbf{X}}]^{\top} \mathbf{y}^*,$$

where " $\stackrel{d}{=}$ " means equivalent in the joint distribution.

Theorem 2.2 shows that the inactive features in \mathbf{X}^* are pairwise exchangeable with their GKnockoff counterparts in terms of the inner product with the response variable. Under Gaussian assumption, the swapped distribution is

$$[\mathbf{X}^*, \tilde{\mathbf{X}}]_{\text{swap}(\mathcal{G})}^{\top} \mathbf{y}^* \sim N([\mathbf{X}^*, \tilde{\mathbf{X}}]_{\text{swap}(\mathcal{G})}^{\top} \mathbf{X}^* \boldsymbol{\theta}_1, \sigma^2 [\mathbf{X}^*, \tilde{\mathbf{X}}]_{\text{swap}(\mathcal{G})}^{\top} \mathbf{M}_{\mathbf{X}\mathbf{F}} [\mathbf{X}^*, \tilde{\mathbf{X}}]_{\text{swap}(\mathcal{G})}^{\top}). \tag{2.11}$$

Then the pairwise exchangeability would hold only if the expectation and covariance of swapped distribution are invariant. The invariance of expectation results from the fact that $\theta_{1j} = 0$ for $j \in \mathcal{S}^c$. The invariance of covariance, on the other hand, is a bit tricky and relies on Lemma A.1, which states that a projection of $\tilde{\mathbf{X}}$ is also a Gknockoff of \mathbf{X}^* . We refer to Appendix A.3 for a detailed proof of Theorem 2.2.

The pairwise exchangeability motives us to extend (2.6) to an augmented regularized regression problem

$$\min_{\boldsymbol{\theta}_1 \in \mathbb{R}^m, \tilde{\boldsymbol{\theta}}_1 \in \mathbb{R}^m} \frac{1}{2} \|\mathbf{y}^* - \mathbf{X}^* \boldsymbol{\theta}_1 - \tilde{\mathbf{X}} \tilde{\boldsymbol{\theta}}_1 \|_2^2 + \lambda (\|\boldsymbol{\theta}_1\|_1 + \|\tilde{\boldsymbol{\theta}}_1\|_1). \tag{2.12}$$

The regularization parameter λ controls the sparsity level along the solution path of (2.12): A larger λ detects less structural changes as it shrinks more estimated coefficients to zero and vice versa. Intuitively, an active feature that represents a structural change should enter the solution path of (2.12) earlier than its Gknockoff counterpart; in contrast, inactive features may behave similarly to their Gknockoff counterparts.

Denote $[\hat{\boldsymbol{\theta}}_1^{\top}(\lambda), \tilde{\boldsymbol{\theta}}_1^{\top}(\lambda)]^{\top} \in \mathbb{R}^{2m}$ the minimizer of (2.12), where $\hat{\boldsymbol{\theta}}_1(\lambda) = [\hat{\theta}_{11}(\lambda), \ldots, \hat{\theta}_{1m}(\lambda)]^{\top} \in \mathbb{R}^m$ and $\tilde{\boldsymbol{\theta}}_1(\lambda) = [\tilde{\theta}_{11}(\lambda), \ldots, \tilde{\theta}_{1m}(\lambda)]^{\top} \in \mathbb{R}^m$. Let λ_j and $\tilde{\lambda}_j$ be the values of λ such that the jth feature and its GKnockoff counterpart first enters the solution path of (2.12), respectively. In other

words, we have

$$\lambda_j = \sup\{\lambda : \hat{\theta}_{1j}(\lambda) \neq 0\}, \quad \tilde{\lambda}_j = \sup\{\lambda : \tilde{\theta}_{1j}(\lambda) \neq 0\}.$$

Furthermore, we define a vector of GKnockoff statistics $\mathbf{w} = [W_1, \ \dots, \ W_m]^{\top}$ with

$$W_j = (\lambda_j \vee \tilde{\lambda}_j) \cdot \operatorname{sign}(\lambda_j - \tilde{\lambda}_j), \quad j = 1, \dots, m.$$
(2.13)

Note that the construction of GKnockoff statistics is not unique and here we only exhibit one possibility as in (2.13). A large positive value of $|W_j|$ provides some evidence that \mathbf{y}^* depends on the jth column of \mathbf{X}^* and hence the jth feature may indicate a true structural change. On the other hand, when the jth feature is inactive, W_j should be close to 0 and is equally likely to be positive or negative. This intuition is justified by the following lemma.

Lemma 2.1. Let $\boldsymbol{\xi} = [\xi_1, \dots, \xi_m]^{\top}$ be an indicator sequence independent of \mathbf{w} , where $\xi_j = 1$ if $j \in \mathcal{S}$ and ξ_j is independently drawn from Bernoulli(0.5) if $j \in \mathcal{S}^c$. Then, we have

$$[W_1, \dots, W_m]^{\top} \stackrel{d}{=} [W_1 \xi_1, \dots, W_m \xi_m]^{\top}.$$

Lemma 2.1 is a direct consequence of the pairwise exchangeability of GKnockoff features. The proof of Lemma 2.1 is similar to that of Lemma 1 in Barber and Candès (2015), and hence is omitted. With the results in Lemma 2.1, we have the following conservative approximation for the number of false discoveries

$$|\{j \in \mathcal{S}^c : W_j \ge t\}| \approx |\{j \in \mathcal{S}^c : W_j \le -t\}| \le |\{j : W_j \le -t\}|.$$

To control FDR at a pre-specified level $q \in [0, 1]$, we follow the knockoff+ procedure (Barber and Candès, 2015) and choose a cutoff T(q) as

$$T(q) = \min \left\{ t \in \mathcal{W} : \frac{1 + |\{j : W_j \le -t\}|}{|\{j : W_j \ge t\}| \lor 1} \le q \right\},$$
 (2.14)

where $\mathcal{W}=\{|W_1|:j=1,\ \dots,\ m\}/\{0\}$ and the extra term 1 in the numerator makes the choice of

T(q) slightly more conservative. Naturally, we estimate the active set \mathcal{S} by

$$\hat{S} = \{ j = 1, \dots, m : W_j \ge T(q) \}.$$
 (2.15)

Throughout this paper, we use GKnockoff filter to name the entire procedure of constructing the GKnockoff features $\tilde{\mathbf{X}}$, computing the GKnockoff statistics \mathbf{w} , choosing the cutoff T(q), and estimating the active set by $\hat{\mathcal{S}}$. The following main theorem proves the GKnockoff filter can control FDR at any pre-specified level.

Theorem 2.3. For any $q \in [0,1]$, the active set estimated by the GKnockoff filter, i.e. \hat{S} defined in (2.15), satisfies

$$FDR(q) = \mathbb{E}\left[\frac{|\hat{S} \cap S^c|}{|\hat{S}|}\right] \le q.$$
 (2.16)

When m < n < 2m, we can no longer compute the GKnockoff features $\tilde{\mathbf{X}}$ from (2.10) since it is beyond hope to find a subspace of dimension m that is orthogonal to \mathbf{X}^* , and hence neither $\tilde{\mathbf{U}}$. To address this issue, we create 2m - n dummy observations and extend (2.7) to the following augmented probability model

$$\left[\begin{array}{c} \mathbf{y}^* \\ \mathbf{y}_a^* \end{array}\right] \sim N \left(\left[\begin{array}{c} \mathbf{X}^* \\ \mathbf{0}_{(2m-n) \times m} \end{array}\right] \boldsymbol{\theta}_1, \sigma^2 \left[\begin{array}{c} \mathbf{M}, & \mathbf{0} \\ \mathbf{0}, & \mathbf{I}_{(2m-n)} \end{array}\right]\right).$$

To distinguish with the GKnockoff filter introduced above, we name the GKnockoff filter based on this row-augmented data as the Extended Generalized Knockoff (EGKnockoff) filter. Theorem 2.4 proves that the EGKnockoff filter can also control FDR at any pre-specified level.

Theorem 2.4. Denote $\hat{S}_E := \hat{S}_E(q)$ the active set estimated by the EGKnockoff filter with any pre-specified level $q \in [0,1]$. Then we have

$$FDR_E(q) = \mathbb{E}\left[\frac{|\hat{S}_E \cap S^c|}{|\hat{S}_E|}\right] \le q.$$
 (2.17)

The proof of Theorem 2.4 is presented in Appendix A.5. The EGKnockoff filter requires the sample size n to be larger than the number of features m since we need to estimate the unknown parameter σ from the sample. In the next section, we propose a two-step procedure to address the

high-dimensional (i.e. $m \ge n$) structural change detection and FDR control problem.

3 High-dimensional structural change detection

The GKnockoff and EGKnockoff filters require n > m and hence are not applicable to high-dimensional scenarios where $n \le m$. In this section, we study high-dimensional structural change detection with FDR control and propose a two-stage procedure. We first implement a screening method to filter out a substantial number of locations where the structural changes are unlikely to exist. Then, we apply GKnockoff to the low-dimensional screened data.

3.1 Fused sure independence screening

In this subsection, we use the piecewise constant coefficients profile model (Scenario 2 in Section 2) as a showcase example to introduce a screening strategy for high-dimensional structural change detection problems. Recall that in this scenario, we assume the p coefficients β_1, \ldots, β_p can be segmented into J+1 groups and $\mathcal{S} = \{\tau_1, \ldots, \tau_J\}$ is the active set of all structural change locations. Denote X_j as the standardized jth column of \mathbf{X} and $\hat{\gamma}_j = X_j^{\mathsf{T}} \mathbf{y}$. Then, we define a fused screening statistic to quantify the structural change before and after a location by incorporating the information in a small neighborhood, i.e.

$$\hat{D}(j,h) = \frac{1}{h} \sum_{i=1}^{h} |\hat{\gamma}_{j-i+1} - \hat{\gamma}_{j+i}|, \quad j = h, \dots, p - h,$$
(3.1)

where h > 0 is a bandwidth parameter. We would expect $\hat{\mathbf{D}}(j,h)$ to be large if $j \in \mathcal{S}$ and $\hat{\mathbf{D}}(j,h)$ to be small if there is no structural change within $\{j-h+1, \ldots, j+h\}$.

We propose to screen out the locations whose fused screening statistics are small. For a prespecified threshold $\vartheta > 0$, we can select a screened set as

$$\hat{\mathcal{A}}(\vartheta) = \{j = 1, \ldots, p - 1 : \hat{\mathcal{D}}(j, h) \ge \vartheta\}.$$

The screening procedure is thereby named Fused Sure Independence Screening (FuSIS). Next, we

show FuSIS enjoys a sure screening property under mild conditions, which means \hat{A} contains all structural changes with a probability approaching 1. To start with, we define the population fused screening statistic $D(j,h) = \frac{1}{h} \sum_{i=1}^{h} |\gamma_{j-i+1} - \gamma_{j+i}|$, and introduce two conditions.

Condition 3.1. $\min_{j \in \mathcal{S}} D(j,h) \ge 2c_3 n^{-\kappa}$ for some constants $c_3 > 0$ and $0 \le \kappa \le 1/2$.

Condition 3.2. All structural change locations lie in $\{h, \ldots, p-h\}$.

Condition 3.1 is a widely used minimum signal strength condition in screening literature (e.g. Liu et al., 2021). This condition is mild since it allows the minimum signal strength slowly decays to 0 as the sample size diverges. Condition 3.2 assumes the change points should not lie too close to the boundaries, which is common for change point detection (e.g. Niu and Zhang, 2012). In practice, Condition 3.2 can be satisfied by considering the observations near the boundaries as "burn-in" and "burn-out" samples where we do not detect structural changes.

Theorem 3.1 (Sure screening property). Under Conditions 3.1 and 3.2, let $\vartheta \leq \min_{j \in \mathcal{S}} D(j,h)/2$, we have

$$\Pr(\mathcal{S} \subset \widehat{\mathcal{A}}(\vartheta)) \ge 1 - O\left(hJ\exp\left\{-c_4 n^{1-2\kappa}\right\}\right),\tag{3.2}$$

where $c_4 > 0$ is a positive constant and J = |S|.

The proof of Theorem 3.1 is given in Appendix A.6.

3.2 Bandwidth Selection

The bandwidth parameter h plays an essential role in FuSIS. Next, we introduce a data-driven bandwidth selection procedure. Let h_1, \ldots, h_B be a sequence of grid points. For a given grid point h_k , $k = 1, \ldots, B$, denote $\hat{\mathcal{A}}_k(\vartheta) = \{\hat{\tau}_{k1}, \ldots, \hat{\tau}_{k\hat{J}_k}\}$ the set screened by FuSIS with the bandwidth h_k , where $\hat{J}_k = |\hat{\mathcal{A}}_k(\vartheta)|$. The set $\hat{\mathcal{A}}_k(\vartheta)$ naturally divide the features in \mathbf{X} into $\hat{J}_k + 1$ homogeneous groups, say $\hat{G}_1, \ldots, \hat{G}_{\hat{J}_k+1}$, such that the coefficients share the same value within each group. For each $\hat{\mathcal{A}}_k(\vartheta)$, we can solve a constrained ordinary least squaresl problem

$$\min_{\mathbf{b}\in\mathbb{R}^p} \|\mathbf{y} - \mathbf{X}\mathbf{b}\|_2^2 \text{ subject to } b_1 = \dots = b_{\hat{\tau}_{k1}}; \dots; b_{\hat{\tau}_{k\hat{J}_k}+1} = \dots = b_p.$$

This optimization problem is equivalent to

$$\min_{\boldsymbol{\nu} \in \mathbb{R}^{\hat{J}_k+1}} ||\mathbf{y} - \mathbf{X} \mathbf{Q}_k \boldsymbol{\nu}||_2^2, \tag{3.3}$$

where \mathbf{Q}_k is a $p \times (\hat{J}_k + 1)$ matrix, whose (i, j)th entry equals to 1 if the *i*th feature in \mathbf{X} belongs to \hat{G}_j and 0 otherwise. The solution of (3.3) admits a closed form

$$\hat{oldsymbol{
u}}_k = \left\{ (\mathbf{X}\mathbf{Q}_k)^ op (\mathbf{X}\mathbf{Q}_k)
ight\}^{-1} (\mathbf{X}\mathbf{Q}_k)^ op \mathbf{y}.$$

Further, we can define the R^2 associated with $\hat{\nu}_k$, and hence h_k , as R_k^2 . The empirical optimal bandwidth is defined as

$$h_{opt}(\vartheta) = \arg \max_{h_k \in \{h_1, \dots, h_B\}} R_k^2, \tag{3.4}$$

and the resulting screened set is dentoed as $\hat{\mathcal{A}}_{opt}(\vartheta)$. We summarize the entire FuSIS procedure with bandwidth selection in Algorithm 1.

Algorithm 1 FuSIS with bandwidth selection

- 1: **Input:** Observed data (\mathbf{X}, \mathbf{y}) , bandwidth grid points h_1, \dots, h_B , and a threshold ϑ .
- 2: **FuSIS:** For k = 1, ..., B, apply FuSIS to (\mathbf{X}, \mathbf{y}) with bandwidth h_k . Obtain the kth screened set $\hat{\mathcal{A}}_k(\vartheta)$ and the associated R_k^2 .
- 3: Bandwidth selection: Define the optimal bandwidth as (3.4).
- 4: Output: $\hat{\mathcal{A}}_{opt}(\vartheta)$.

3.3 High-dimensional generalized knockoff

In this subsection, we propose a two-stage procedure named High-dimensional Generalized Knockoff filter (HGKnockoff filter) to detect structural changes in high-dimensional scenarios and control FDR at a pre-specified level. To avoid the mathematical and empirical challenges cased by reusing the data, we adopt a data splitting strategy for the two steps. To be specific, We randomly partition (\mathbf{X}, \mathbf{y}) into two subsamples $(\mathbf{X}^{(1)}, \mathbf{y}^{(1)})$ and $(\mathbf{X}^{(2)}, \mathbf{y}^{(2)})$ with sample sizes n_1 and $n_2 = n - n_1$, respectively.

The two stages of the HGKnockoff filter are introduced as follows:

(1) FuSIS stage: Apply Algorithm 1 to $(\mathbf{X}^{(1)}, \mathbf{y}^{(1)})$ with a threshold ϑ such that the screened

set $\hat{\mathcal{A}}_{opt}(\vartheta)$ contains less than $n_2/2$ elements, i.e. $|\hat{\mathcal{A}}_{opt}(\vartheta)| < n_2/2$.

(2) GKNOCKOFF STAGE: Denote $\mathbf{X}_{\text{FuSIS}}^{(2)}$ the sub-matrix of $\mathbf{X}^{(2)}$ whose column corresponding to $\hat{\mathcal{A}}_{opt}(\vartheta)$. Then, we apply the GKnockoff filter to $(\mathbf{X}_{\text{FuSIS}}^{(2)}, \mathbf{y}^{(2)})$ to detect structural changes while controlling FDR at a pre-specified level q. The final estimator of the active set is denoted as $\hat{\mathcal{S}}_H := \hat{\mathcal{S}}_H(\vartheta, q)$.

In Theorem 3.2 below, under mild conditions, we prove the HGKnockoff filter can control FDR at any pre-specified $q \in [0, 1]$.

Theorem 3.2. (a) Under Conditions 3.1 and 3.2, for any $q \in [0, 1]$, the HGKnockoff filter satisfies

$$FDR_H(q) = \mathbb{E}\left[\frac{|\mathcal{S}^c \cap \hat{\mathcal{S}}_H|}{|\hat{\mathcal{S}}_H|}\right] \le q$$
 (3.5)

with a probability approaching 1 as $n \to \infty$.

(b) Furthermore, conditional on the sure screening event $\mathcal{E} = \{\mathcal{S} \subset \hat{\mathcal{A}}_{opt}(\vartheta)\}$, we can get a finite sample guarantee of FDR control

$$FDR_H(q) = \mathbb{E}\left[\frac{|\mathcal{S}^c \cap \hat{\mathcal{S}}_H|}{|\hat{\mathcal{S}}_H|}\Big|\mathcal{E}\right] \le q.$$
 (3.6)

4 Simulation Studies

In this section, we simulate various structural change detection experiments to evaluate the empirical performance of GKnockoff, FuSIS, and HGKnockoff. We also compare the proposed methods with some popular competitors in the literature.

4.1 Simulations for the GKnockoff filter

We apply the GKnockoff filter to study the three structural change detection scenarios discussed in Section 2.1. We also apply the B-Y method (Benjamini and Yekutieli, 2001) and the classical permutation-based method to these scenarios for comparison purpose. Throughout this subsection, we set the error variance $\sigma^2 = 1$, $\mathbf{X} = (\mathbf{x}_1, \dots, \mathbf{x}_n)^{\top}$, and draw \mathbf{x}_i 's independently from $N(\mathbf{0}, \mathbf{\Sigma}_{p \times p})$

where $\Sigma_{(i,j)} = \rho^{|i-j|}$ for some $\rho \in [0,1)$. The nominal FDR level is fixed to be q = 0.2. The active set of structural change locations is set to be $S = \{\tau_1, \ldots, \tau_J\}$. We focus on comparing the GKnockoff filter and the B-Y method in terms of the estimated FDR and the empirical power. For each case, we simulate 200 replications. To be specific, the estimated FDR and the empirical Power are defined by

$$\widehat{\text{FDR}} = \frac{1}{200} \sum_{i=1}^{200} \frac{|\hat{\mathcal{S}}_i \cap \mathcal{S}^c|}{|\hat{\mathcal{S}}|} \quad \text{and} \quad \widehat{\text{Power}} = \frac{1}{200} \sum_{i=1}^{200} \frac{|\hat{\mathcal{S}}_i \cap \mathcal{S}|}{|\mathcal{S}|},$$

where \hat{S}_i is the active set estimated by either the GKnockoff filter or the B-Y method in the *i*th replication. We will also discuss the permutation-based method at the end of this subsection, and show that it fails to control FDR in our simulations settings.

Experiment 4.1: Change points detection

Consider the normal mean MCM model in Scenario 1. We set n=350. The true mean parameters are set to be

$$\mu_{\tau_{k-1}+1} = \cdots = \mu_{\tau_k} = (-1)^k A$$
, for $k = 1, \ldots, J$,

where A is a positive parameter that controls the signal amplitude and we denote $\tau_0 = 0$. We design the signal amplitude A and the number of change points J in the following fashion.

- (1) Fix A = 2.5 and let J vary in $\{6, 7, 8, 9, 10, 11\}$.
- (2) Fix J = 10 and let A vary in $\{1.8, 2.0, 2.2, 2.4, 2.6, 2.8\}$.

Figure 1 summarizes the estimated FDR and the empirical power with a fixed A and an increasing J. We observe that both methods can control FDR under the pre-specified level and the empirical powers increase with J. The GKnockoff filter has higher empirical powers than the B-Y method in all cases. Figure 2 summarizes the estimated FDR and the empirical power with a fixed J and an increasing A. Again, both methods can control FDR under the pre-specified level and the GKnockoff filter outperforms the B-Y method in terms of empirical powers.

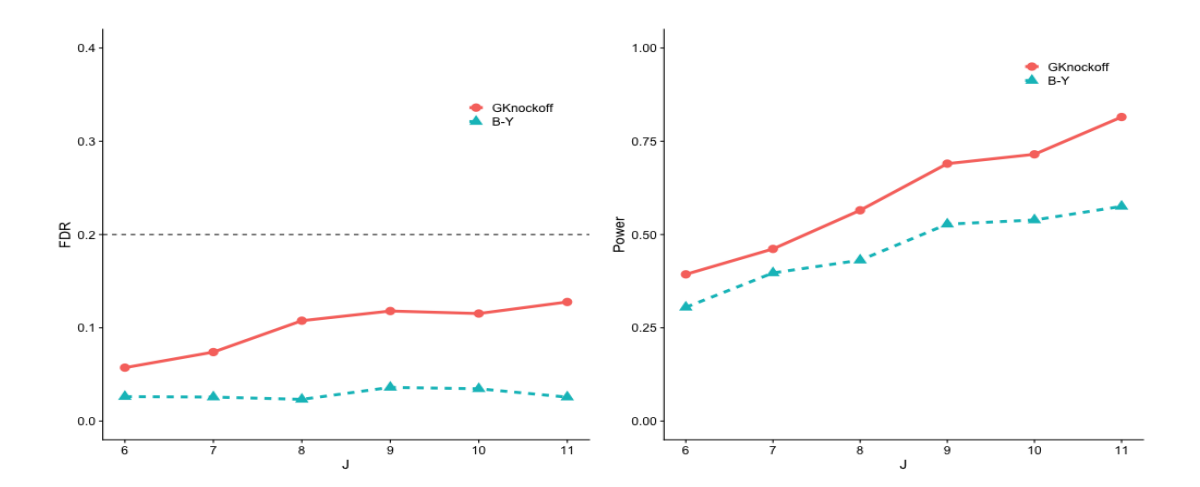


Figure 1: FDR and power with respect to J for GKnockoff and B-Y in Experiment 4.1.

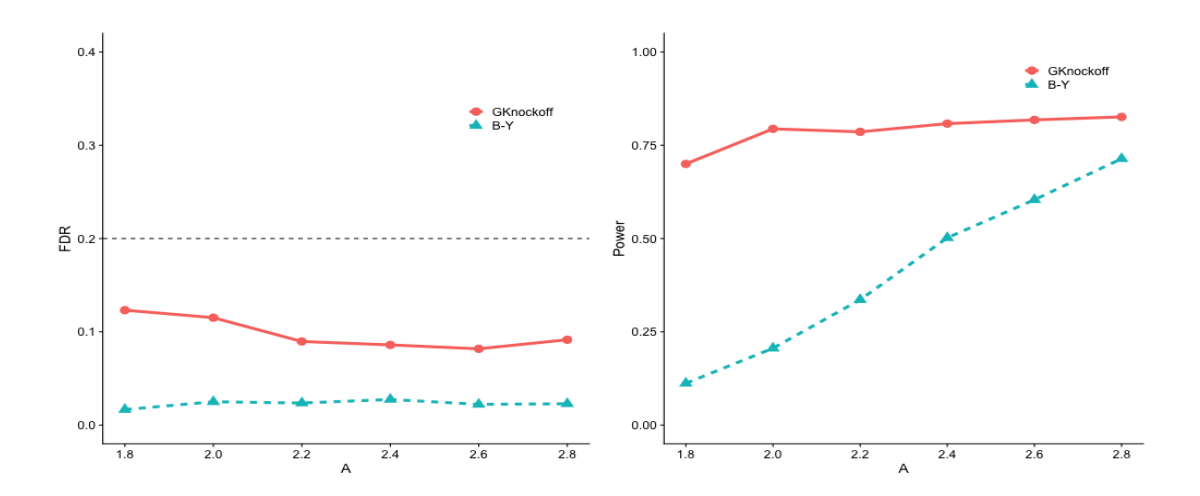


Figure 2: FDR and power with respect to A for GKnockoff and B-Y in in Experiment 4.1.

Experiment 4.2: Piecewise constant coefficients profile

Consider the piecewise constant coefficients profile model in Scenario 2. We set n=350 and p=100. The true coefficients are set to be

$$\beta_{\tau_{k-1}+1} = \cdots = \beta_{\tau_k} = (-1)^k A$$
, for $k = 1, \ldots, J$,

where A is a positive parameter that controls the signal amplitude and we denote $\tau_0 = 0$. We choose J, A and the ρ as follows.

(1) Fix A = 0.12, $\rho = 0$, and let J vary in $\{9, 10, 11, 12, 13, 14\}$.

- (2) Fix J = 13, $\rho = 0$, and let A vary in $\{0.09, 0.10, 0.11, 0.12, 0.13, 0.14\}$.
- (3) Fix J = 13, A = 0.12. and let ρ vary in $\{0, 0.06, 0.12, 0.18, 0.24, 0.30\}$.

The simulation results are summarized in Figures 3, 4 and 5. Similar as the previous experiment, both methods can control FDR at the pre-specified level q = 0.2. Regarding the empirical power, the GKnockoff filter uniformly outperforms the B-Y method especially when the signal A is small.

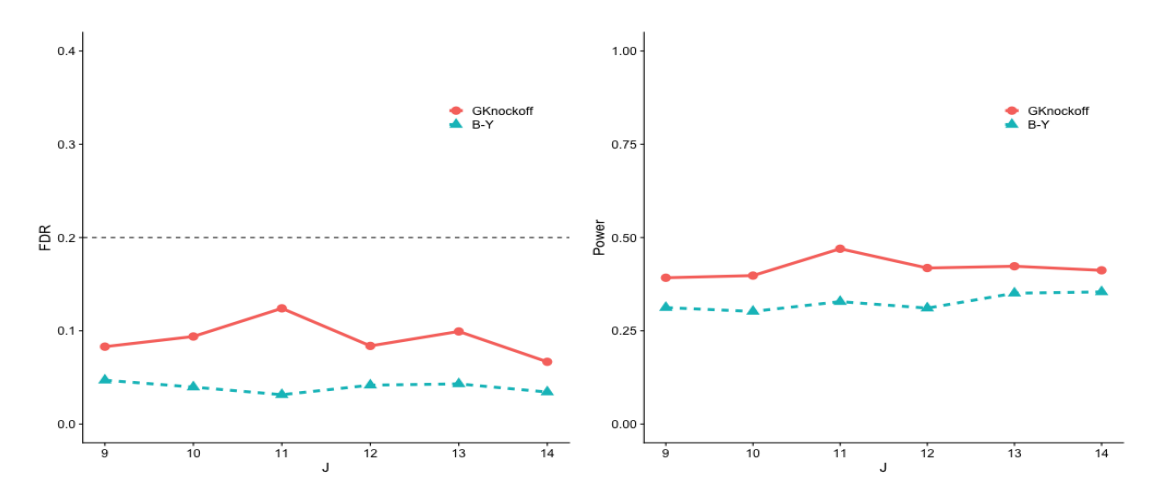


Figure 3: FDR and power with respect to J for GKnockoff and B-Y in Experiment 4.2.

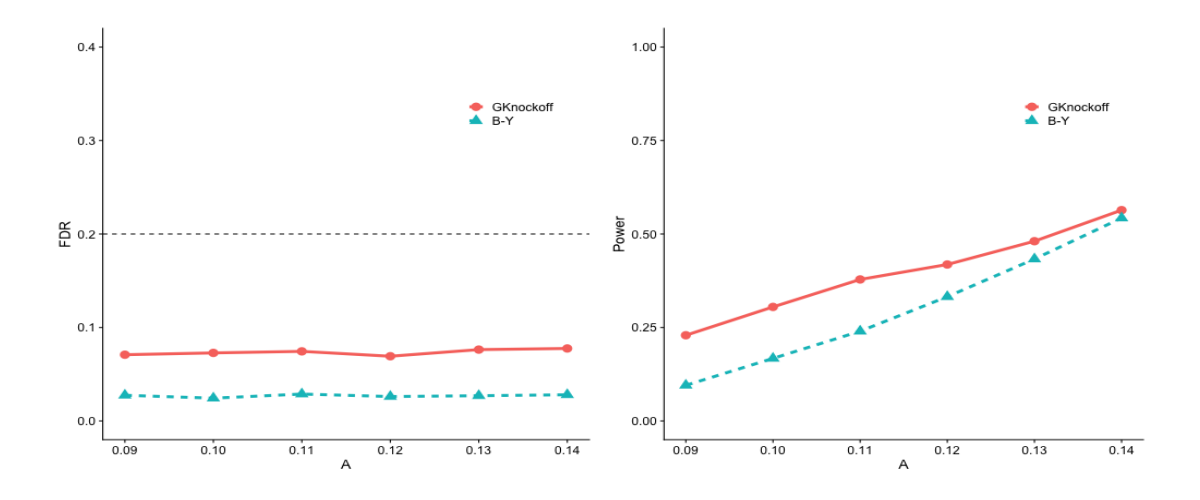


Figure 4: FDR and power with respect to A for GKnockoff and B-Y in Experiment 4.2.

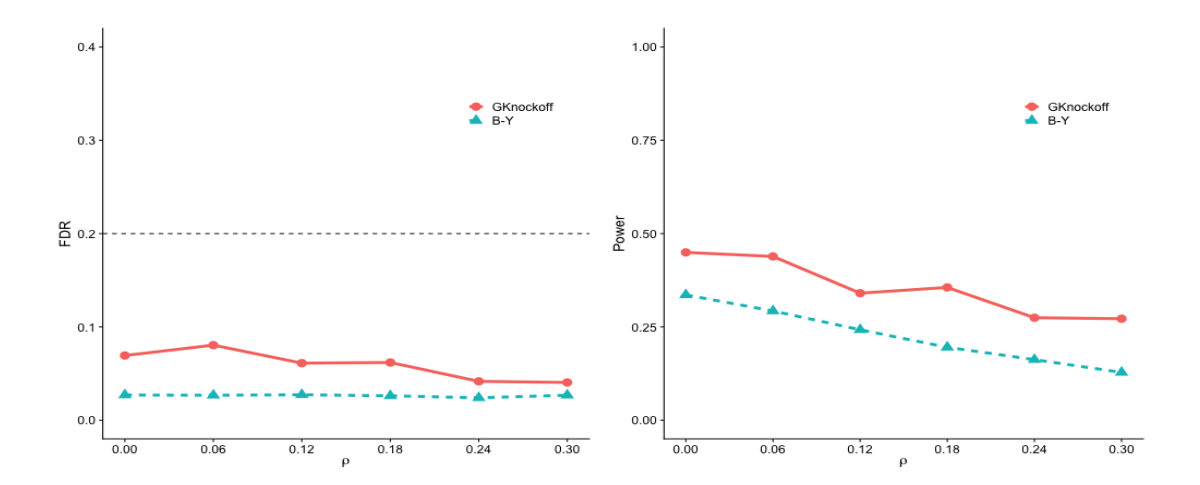


Figure 5: FDR and power with respect to ρ for GKnockoff and B-Y in Experiment 4.2.

Experiment 4.3: Integration analysis from multiple data sources

Consider the integration analysis from K data sources as discussed in Scenario 3. We set p=40. The sample size of the kth source, i.e. $n^{(k)}$, is independently drawn from $Poission(\zeta)$, where $\zeta=100$, for $k=1,\ldots,K$. The number of structural changes J now stands for the total number of distinct coefficients from adjacent data sources. If (k,τ_j) is a change position, we set $\beta_{\tau_j}^{(k)}=-\beta_{\tau_j}^{(k+1)}$. The amplitude A is accordingly defined as $A=|\beta_j^{(k)}|$ for all $k=1,\ldots,K$ and $j=1,\ldots,p$. The ith sample from the kth source $\mathbf{x}_i^{(k)}$ is independently generated from $N(0,\mathbf{I}_p), i=1,\ldots,n_k$ and $k=1,\ldots,K$. Further, we choose K, K and K as follows.

- (1) Fix K = 5, A = 0.25, and let J vary in $\{15, 17, 19, 21, 23, 25\}$.
- (2) Fix J = 20, A = 0.25, and let K vary in $\{3, 4, 5, 6, 7, 8\}$.

The simulation results are summarized in Figures 6 and 7. Again, both methods can successfully control FDR at the pre-specified level q = 0.2, and the GKnockoff filter gains significantly more empirical power than the B-Y method.

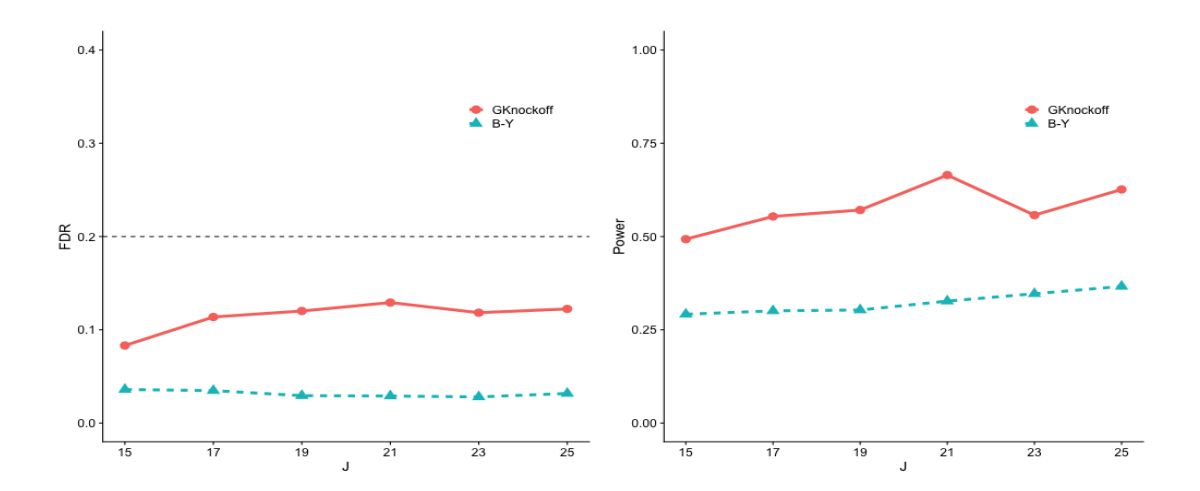


Figure 6: FDR and power with respect to J for GKnockoff and B-Y in Experiment 4.3.

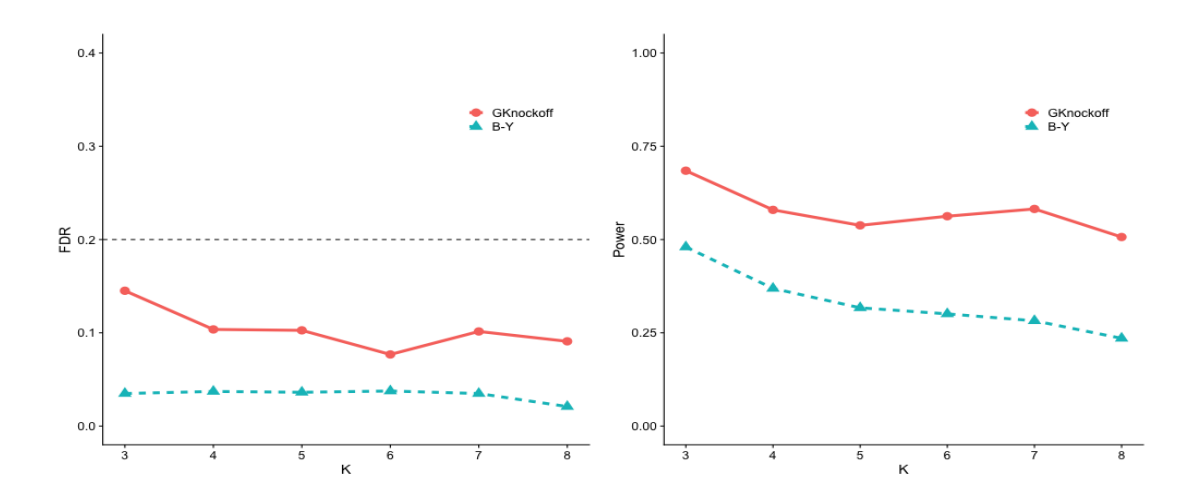


Figure 7: FDR and power with respect to K for GKnockoff and B-Y in Experiment 4.3.

Next, we compare the FDR control performance of the Gknockoff filter with a permutation-based method in all three experiments studied above. The permutation-method constructs "knockoff" of \mathbf{X}^* by randomly permuting its rows. For Experiment 4.1, we set n=350, A=1.8 and J=12. For Experiment 4.2, we set n=350, p=100, A=0.1, J=10 and $\rho=0$. For Experiment 4.3, we set $\zeta=100$, p=40, A=0.25, K=5, J=20 and $\rho=0$. Table 1 reports the estimated FDR of the two methods, which shows the permutation-based method fails to control FDR at q=0.2 for all three structural change problems. We argue that the permutation-based method, though straightforward, can not address the dependence in the noise $\mathbf{M}\boldsymbol{\epsilon}$ and hence does not enjoy the pairwise exchangeability.

Table 1: Estimated FDR by permutation and GKnockoff

	Change points	piecewise constant coefficients	Integration analysis
Permutation	0.542	0.611	0.595
GKnockoff	0.112	0.096	0.122

4.2 Simulations for FuSIS

In this subsection, we use simulated experiments to assess the finite sample performance of FuSIS for screening coefficient changes in Experiment 4.2. Within each replication, we compute and rank $\hat{\mathbf{D}}(h,j)$ in a descending order and choose the first n-1 locations as the selection set $\hat{\mathcal{A}}$. We set sample size and dimensionality to be $(n,p)=(300,\ 1000)$ and $(n,p)=(1500,\ 10000)$. The active set of structural change locations is set to be $\mathcal{S}=\left\{\frac{p}{10},\frac{2p}{10},\ldots,\frac{9p}{10}\right\}$ with J=9, and the signal amplitude A=0.1. The covariates, i.e. \mathbf{x}_i 's, are independently drawn from $N(\mathbf{0},\mathbf{\Sigma})$, where $\mathbf{\Sigma}$ admits one of the following two forms.

- (1) $(AR \ structure) \ \Sigma_{(i,j)} = \rho^{|i-j|}, \ i,j=1, \ \dots, \ p.$
- (2) (*Group structure*) Σ is a block diagonal matrix, with ten $\frac{p}{10} \times \frac{p}{10}$ dimensional matrices on the diagonal, each of which is defined as $\Sigma^{(0)}$, where $\Sigma^{(0)}_{(i,j)} = \rho^{|i-j|}$, $i, j = 1, \ldots, \frac{p}{10}$.

We take $\rho = 0.3$, 0.6 and 0.9, respectively. Based on 1000 simulation replications, we assess the sure screening property of FuSIS via the coverage proportion of all true coefficient change locations. For bandwidth selection, we demonstrate two methods: (a) a fixed bandwidth that is chosen such that at most one change occurs within each h-neighborhood; specifically, h = 25 when p = 1000, and h = 100 when p = 10000; (b) an optimal bandwidth selected by the data-driven bandwidth method introduced in Section 3.2. The results are reported in Table 2, from which one can see that the coverage proportions are all close to 1. In addition, the optimal bandwidth generally yields a larger coverage rate than the fixed bandwidth.

Table 2: Coverage proportion of FuSIS

		p = 1000, n = 300		p = 10000, n = 1500		
	ρ	Fixed h	Optimal h	Fixed h	Optimal h	
	0.3	0.886	0.918	0.918	0.942	
AR structure	0.6	0.958	0.964	0.964	0.983	
	0.9	0.966	0.983	0.971	1	
	0.3	0.876	0.927	0.917	0.974	
Group structure	0.6	0.933	0.966	0.966	1	
	0.9	0.972	0.982	0.982	1	

4.3 Simulations for the HGKnockoff filter

In this subsection, we access the performance of the HGKnockoff filter for a high-dimensional piecewise constant coefficients profile model. Note that the B-Y method is not applicable when p > n, and hence we adopt the same data splitting technique to first screen the potential structural changes and then apply the B-Y method to the screened features. We name this method the screened B-Y method. In addition, we also consider the sequential B-H method (G'Sell et al., 2016) as a competitor.

We follow a similar simulation setup as in Section 4.2 except for the following aspects. We set n = 900, p = 1000, A = 0.15, and J = 8. We vary ρ from 0.1 to 0.3 for the AR structure, and from 0.4 to 0.6 for the group structure. The sample is randomly partitioned into two halves, one for FuSIS and the other one for structural change detection with FDR control. The simulation results, measured by the estimated FDR and the empirical power, are summarized in Figures 8 and 9. We observe that the sequential B-H method fails to control FDR at the pre-specified level q = 0.2, partly due to the simulation setup violates the independence assumption. The screened B-Y method also does not control FDR well, especially for the AR structure setting. In contrast, the HGknockoff filter controls FDR at q = 0.2. Moreover, the HGknockoff filter has the highest empirical power among the three competitors. Notably, the power trends of HGknockoff behave like inverted-U curves, which reflect the trade-off between controlling FDR and satisfying the sure

screening property.

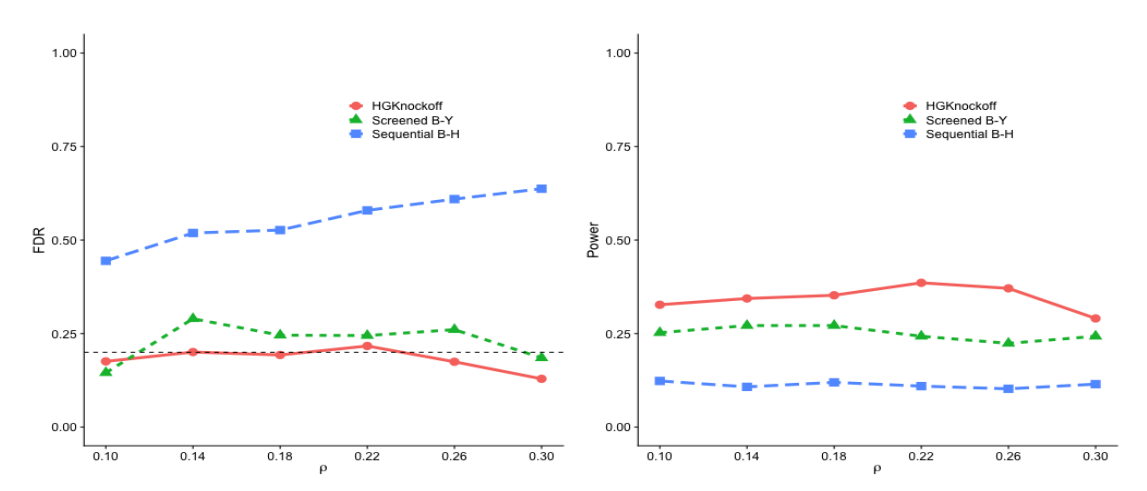


Figure 8: FDR and power trend of HGK nockoff, screened B-Y and sequential B-H with respect to ρ for high-dimensional piecewise constant coefficients profile model under AR structure.

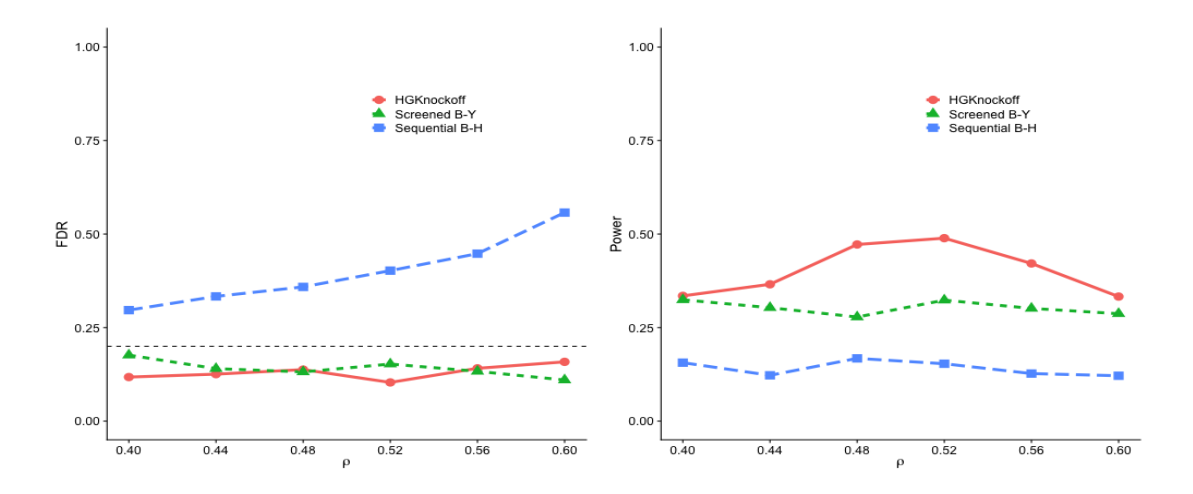


Figure 9: FDR and power trend of HGK nockoff, screened B-Y and sequential B-H with respect to ρ for high-dimensional piecewise constant coefficients profile model under group structure.

5 Real Data Analysis: Change Points Detection for CPI and Unemployment Rate

In this section, we apply the proposed GKnockoff filter to a U.S. macroeconomic dataset, aiming to detect change points of the consumer price index (CPI) and the unemployment rate from January

2000 to January 2021. The monthly CPI and unemployment rate data are collected from the St.Louis Federal Reserve Bank website². CPI, a measure for calculating inflation, records the average change in price over time that consumers pay for a basket of goods and services. The unemployment rate, on the other hand, reflects the labor demand of the country. In this work, we use the GKnockoffs filter to detect the change points of CPI as well as the change points of the unemployment rate. As the strong correlation between inflation and unemployment rate is evidently revealed by the well-known Philips curve, we expect mostly concordant change points, and the distinct discoveries are possibly false discoveries.

We first draw time series plots for the monthly CPI and the monthly unemployment rate in Figure 10. The clear linear increasing trend of CPI motives us to model the monthly CPI as

$$y_{cpi,t} = \delta t + a_t + \epsilon_t \tag{5.1}$$

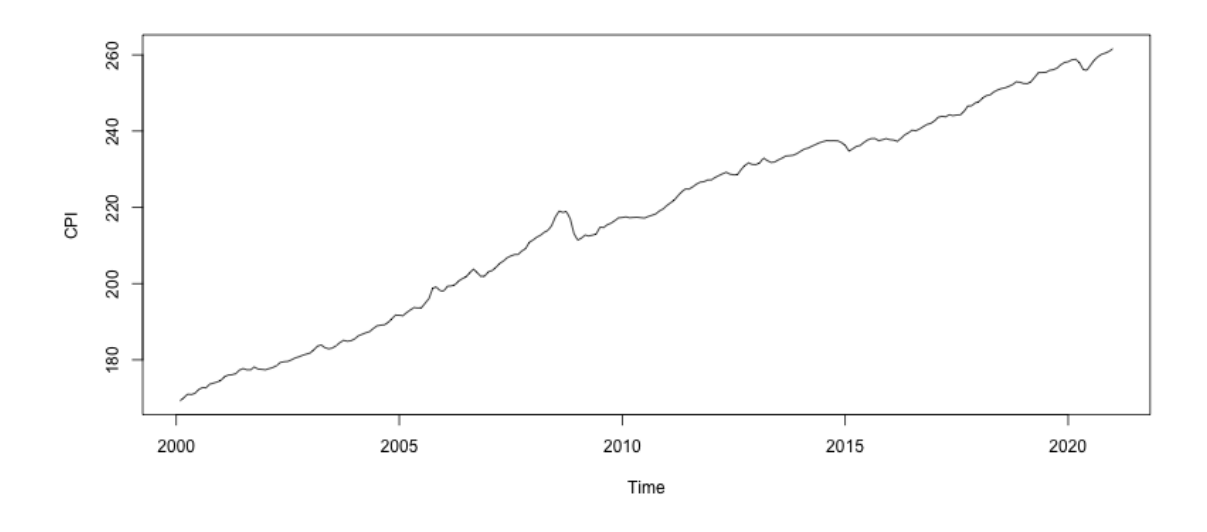
where δ is the effect of time, a_t is the mean effect, and $\epsilon_t \sim N(0, \sigma_1^2)$ is a white noise. Here we focus on detecting the structural changes in the mean effect a_t and assume σ_1^2 is not time-varying for simplicity. The index set of the true mean effect change locations for CPI is defined as $S_{cpi} = \{t = 1, ..., p - 1 : a_{t+1} - a_t \neq 0\}.$

On the other hand, as we do not observe a clear time trend for the unemployment rate data, we model it as

$$y_{unemp,t} = b_t + \gamma_t \tag{5.2}$$

where b_t is the mean effect, and $\gamma_t \sim N(0, \sigma_2^2)$ is a white noise. Similarly, we focus on detecting the structural changes in the mean effect b_t and assume σ_2^2 is not time-varying. The index set of the true mean effect change locations for the unemployment rate is defined as $S_{unemp} = \{t = 1, \dots, p-1: b_{t+1} - b_t \neq 0\}$.

²https://fred.stlouisfed.org



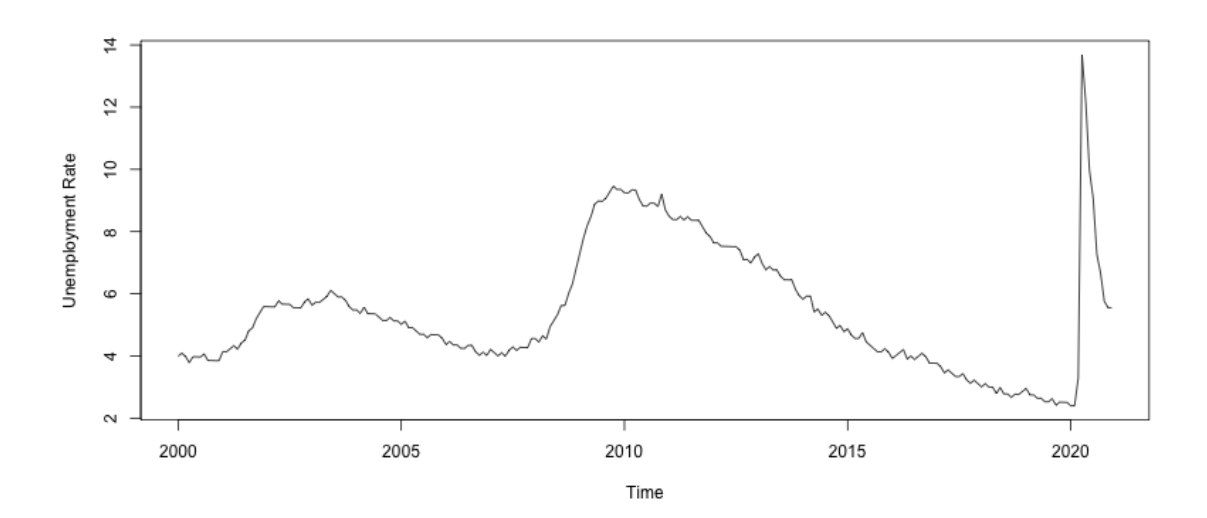


Figure 10: Time series plot for the monthly CPI and monthly unemployment rate in the U.S. between January 2000 and January 2021.

Then, we can apply the GKnockoff filter to both models under a pre-specified FDR level q = 0.2. The estimates of the mean effects change location sets, denoted as $\hat{\mathcal{S}}_{cpi,GK}$ and $\hat{\mathcal{S}}_{unemp,GK}$, are visualized in Figure 11 and listed as follows.

 $\hat{S}_{cpi,GK} = \{09/2005, 11/2007, 06/2008, 10/2008, 11/2008, 12/2008, 12/2014, 03/2020\},$ $\hat{S}_{unemp,GK} = \{11/2007, 04/2008, 07/2008, 09/2008, 11/2008, 01/2009, 03/2009, 03/2014,$

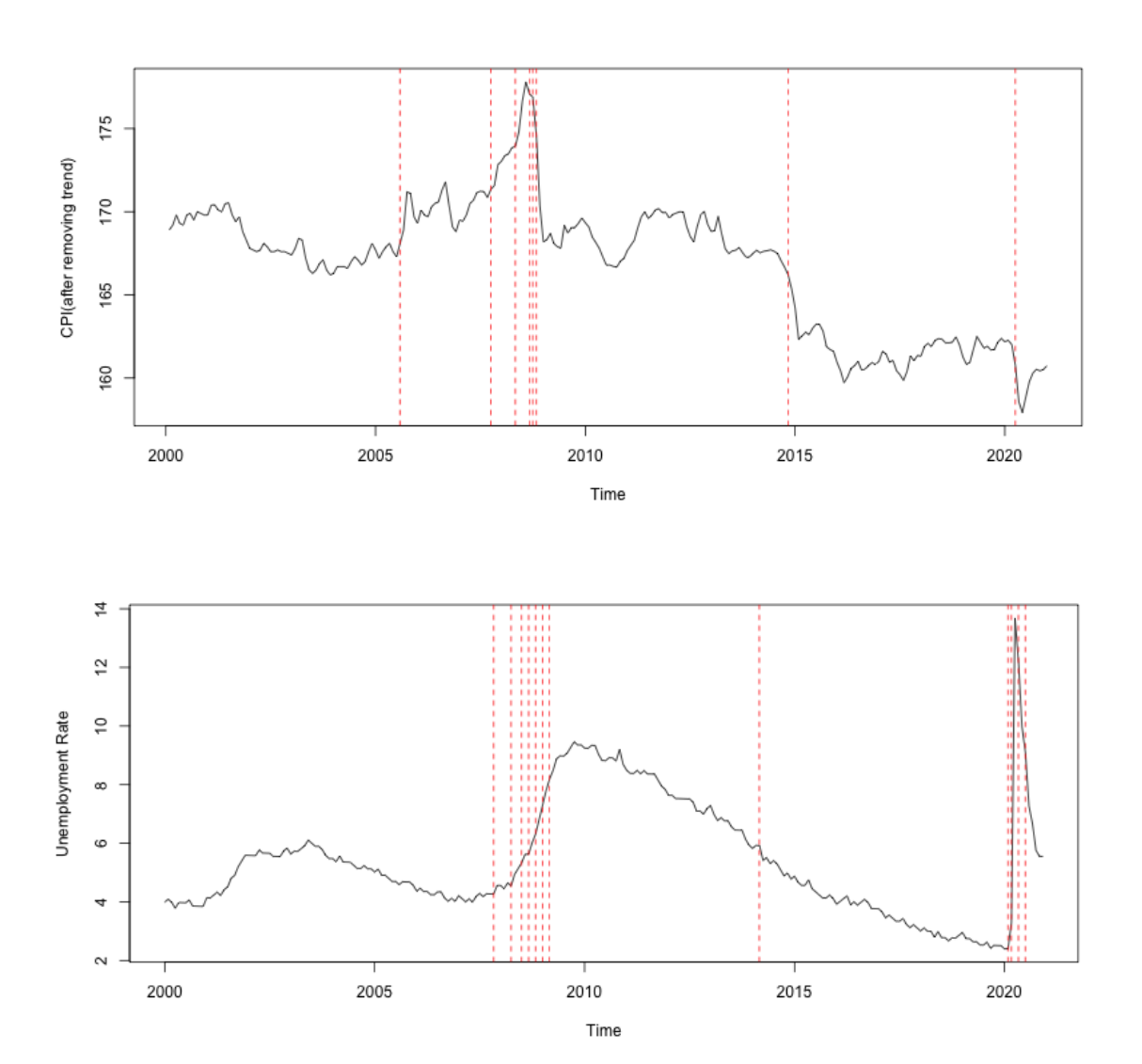


Figure 11: Change point detection for CPI and unemployment rate under nominal level q=0.2 using GKnockoff.

According to Figure 11, it is not surprised that the two time series share many common mean effects change points, say between 2007 and 2008 and in early 2020. There is a well-known global financial crisis between 2007 and 2008 centered in the U.S., which has caused a severe worldwide economic recession and significant damages to financial institutions, real estate, and many other

industries. During that financial crisis, many U.S. companies paused hiring and laid off the employees as they faced stagnant revenues and increased pressures to pay their debts. As a result, the U.S.
unemployment rate rose rapidly during that period of time. The monthly CPI data, after removing
the time trend, also significantly increased during the financial crises but decreased after October
2008. This may be attributed in part to the fact that the Federal Reserve Bank has launched four
rounds of Quantitative Easing (QE) to fight the financial crisis in 2008. The QE mainly enhanced
the financial liquidity by pulling down interest rates. It stimulated the borrowing and spending
activities and gradually brought CPI back to normal. Another pack of change points occurred in
early 2020 because of the COVID-19 pandemic. The breakout of COVID-19 has led to severe global
economic recessions in many countries. Besides, policies like social distancing and lock-down may
boost the unemployment rate in the U.S. Therefore, we see a huge jump in the unemployment rate
in February 2020. After May 2020, the U.S. government began to unlock the cities and encouraged
people back to work. This may lead to a decrease in the unemployment rate.

The discovered mean effect change points for CPI and the unemployment rate are mostly in accordance up to a small neighborhood, which shows the power of a successful FDR control. We also run the generalized Lasso method for both time series without controlling FDR. The estimates of the mean effects change location sets, denoted as $\hat{S}_{cpi,Lasso}$ and $\hat{S}_{unemp,Lasso}$, are listed below. We indeed observe much more discordant change points from the two sets that are likely false discoveries.

 $\hat{\mathcal{S}}_{cpi,Lasso} = \{07/2005, 08/2005, 01/2006, 08/2007, 10/2007, 02/2008, 05/2008, 08/2008, \\ 10/2009, 11/2008, 06/2014, 07/2014, 08/2014, 10/2014, 11/2014, 08/2015, \\ 09/2015, 10/2015, 03/2020, 04/2020\},$

 $\hat{S}_{unemp,Lasso} = \{02/2003, 03/2003, 05/2007, 06/2007, 08/2007, 09/2007, 10/2007, 11/2007, 02/2008, 04/2008, 05/2008, 06/2008, 07/2008, 08/2008, 09/2008, 10/2008, 11/2008, 12/2008, 01/2009, 02/2009, 03/2009, 10/2013, 11/2013, 03/2014, 05/2014, 07/2014, 02/2020, 03/2020, 04/2020, 05/2020, 06/2020, 07/2020\}.$

6 Conclusion

Inspired by a change-point detection problem for CPI and the unemployment rate based on the macroeconomic data in the U.S., we developed a generalized knockoff procedure (GKnockoff) for selecting structural changes while controlling the false discovery rate (FDR). Upon identifying potential structural changes rather than individual features, we adopted the generalized Lasso approach via introducing some full-row-rank transformation matrix for the original coefficient vector. We carefully studied its selection consistency and asymptotic power. The transformed data used in generalized Lasso violates the independence assumption which is crucial to the theoretical guarantees of the classical knockoff. Seeing this, we proposed to construct knockoffs based on the projected design matrix, that accommodates the dependence structure of transformed data. We established the pairwise exchangeability of the GKnockoff design and proved its capability to rigorously control FDR under finite samples. For high-dimensional features, we proposed a new screening technique, called FuSIS, which is of its own significance, that reduces dimensionality by filtering out redundant structural changes. Further, we adopted a data splitting technique, named high-dimensional GKnockoff (HGKnockoff), to first reduce dimensionality and then apply GKnockoff respectively on two halves of data. The sure screening property of FuSIS and the capability of HGKnockoff to control FDR were also proved. Simulation studies empirically verified the outstanding performance of GKnockoff and HGKnockoff in terms of FDR control and power, as well as the sure screening property of FuSIS. We applied the proposed method to analyze a macroeconomic dataset that describes the trend of CPI and the unemployment rate in the U.S. between 2000 to 2021. As expected, the change points of CPI and the unemployment rate are mostly in accordance due to the strong association revealed by the Phillips curve. The inconsistent findings of change points could potentially be considered as a measure of false discoveries. It turns out that the GKnockoff filter indeed yields fewer false discoveries, and is more effective to control FDR in the change-point detection, compared with directly adopting generalized Lasso without GKnockoff involved.

A Appendix

A.1 Some useful lemmas

In this section, we introduce and prove several useful lemmas that facilitate the proposed theories of GKnockoff and FuSIS. The first lemma is established as preparation for the pairwise exchangeability of GKnockoff.

Lemma A.1. Denote the GKnockoff matrix of \mathbf{Z} as $\tilde{\mathbf{Z}}$. For a symmetric matrix \mathbf{M} such that $\mathbf{MZ} = \mathbf{Z}$, $\tilde{\mathbf{Z}}^M = \mathbf{M\tilde{Z}}$ is also a GKnockoff of \mathbf{Z} .

Proof: According to the construction of GKnockoff, $\tilde{\mathbf{Z}} = \mathbf{Z} \left(\mathbf{I} - \mathbf{\Sigma}^{-1} \operatorname{diag}\{\mathbf{s}\} \right) + \tilde{\mathbf{U}}\mathbf{C}$, where $\mathbf{\Sigma} = \mathbf{Z}^{\top}\mathbf{Z}$ and $\tilde{\mathbf{U}}$ is in the null space of \mathbf{Z} . Providing $\mathbf{M}\mathbf{Z} = \mathbf{Z}$,

$$\tilde{\mathbf{Z}}^{M} = \mathbf{M}\tilde{\mathbf{Z}} = \mathbf{M}\mathbf{Z}(\mathbf{I} - \boldsymbol{\Sigma}^{-1}\operatorname{diag}\{\mathbf{s}\}) + \mathbf{M}\tilde{\mathbf{U}}\mathbf{C} = \mathbf{Z}(\mathbf{I} - \boldsymbol{\Sigma}^{-1}\operatorname{diag}\{\mathbf{s}\}) + \mathbf{M}\tilde{\mathbf{U}}\mathbf{C}.$$

In addition, by symmetry of \mathbf{M} , $\mathbf{Z}^{\top}(\mathbf{M}\tilde{\mathbf{U}}) = \mathbf{Z}^{\top}\mathbf{M}^{\top}\tilde{\mathbf{U}} = (\mathbf{M}\mathbf{Z})^{\top}\tilde{\mathbf{U}} = \mathbf{Z}^{\top}\tilde{\mathbf{U}} = 0$, which implies that $\mathbf{M}\tilde{\mathbf{U}}$ is in also the null space of \mathbf{Z} . Hence $\tilde{\mathbf{Z}}^{M}$ is a GKnockoff of \mathbf{Z} .

Next, the following two lemmas serve as building blocks for the sure screening property of FuSIS. Lemma A.2 proves that the Pearson correlation is a U-Statistic. And Lemma A.3 studies the concentration inequality of $\hat{D}(j,h)$.

Lemma A.2. Denote $\{(x_i, y_i), i = 1, ..., n\}$ to be a size-n random sample for the random vector $(X, Y)^{\top}$, and $\bar{x} = \sum_{i=1}^{n} x_i/n$ and $\bar{y} = \sum_{i=1}^{n} y_i/n$. Without loss of generality, all the samples are standardized. Then the Pearson correlation $\widehat{\text{Cor}}(X, Y)$ is a U-Statistic.

Proof: Define a kernel function $h(x_i, x_j, y_i, y_j) = (x_i y_i - x_i y_j + x_j y_j - x_j y_i)/2$. Then the U-statistic specified by function h is

$$U(x) = 1/C_n^2 \cdot \sum_{i < j} h(x_i, x_j, y_i, y_j)$$
(A.1)

Next, we show U(x) is indeed the Pearson correlation.

$$U(x) = \frac{1}{n(n-1)} \sum_{i \neq j} (x_i y_i - x_i y_j)$$

$$= \frac{1}{n(n-1)} \sum_{i,j} (x_i y_i - x_i y_j)$$

$$= \frac{1}{n(n-1)} \sum_{i} (n x_i y_i - x_i \sum_{j} y_j)$$

$$= \frac{1}{n-1} (\sum_{i} x_i y_i - n \bar{x} \bar{y})$$

$$= \widehat{\text{Cor}}(X, Y)$$
(A.2)

That is, the Pearson correlation coefficient is a U-Statistic.

Lemma A.3 below provides the exponential-type deviation inequality for the screening criteria $\hat{D}(j,h)$ which is essential for the sure screening property. The corresponding population quantity is denoted by $D(j,h) = \frac{1}{h} \sum_{i=1}^{h} |\gamma_{j-i+1} - \gamma_{j+i}|$ where γ_j is population covariance $Cov(X_j,Y)$, given that X_j is standardized.

Lemma A.3. For a given bandwidth h and any $0 < \epsilon < 1$, there exists positive constants c_1 and c_2 , such that

$$\Pr\left(|\hat{\mathbf{D}}(j,h) - \mathbf{D}(j,h)| \ge \epsilon\right) \le hc_1 \exp\{-c_2 n\epsilon^2\}. \tag{A.3}$$

Proof: For U-Statistics, Liu et al. (2021) has established the concentration inequality in their Lemma S.1. Together with Lemma A.2, we easily obtain that

$$\Pr(|\hat{\gamma} - \gamma| \ge \epsilon) \le c_1' \exp(-c_2' n \epsilon^2) \tag{A.4}$$

where $\gamma = \operatorname{Cor}(X,Y), \, c_1' > 0$ and $c_2' > 0$ are some positive constant. Note that

$$\Pr\{|\hat{\mathbf{D}}(j,h) - \mathbf{D}(j,h)| \ge \epsilon\} = \Pr\{\hat{\mathbf{D}}(j,h) - \mathbf{D}(j,h) \ge \epsilon, \hat{\mathbf{D}}(j,h) \ge \mathbf{D}(j,h)\}$$

$$+ \Pr\{\mathbf{D}(j,h) - \hat{\mathbf{D}}(j,h) \ge \epsilon, \hat{\mathbf{D}}(j,h) < \mathbf{D}(j,h)\}$$

$$\leq \Pr\{\hat{\mathbf{D}}(j,h) - \mathbf{D}(j,h) \ge \epsilon\} + \Pr\{\mathbf{D}(j,h) - \hat{\mathbf{D}}(j,h) \ge \epsilon\}$$
(A.5)

For the first term of the right hand side in (A.5),

$$\Pr{\{\hat{D}(j,h) - D(j,h) \ge \epsilon\}} = \Pr{\{\frac{1}{h} \sum_{i=1}^{h} |\hat{\gamma}_{j+i-1} - \hat{\gamma}_{j-i}| - \frac{1}{h} \sum_{i=1}^{h} |\gamma_{j+i-1} - \gamma_{j-i}| \ge \epsilon\}}$$

$$= \Pr{\{\sum_{i=1}^{h} (|\hat{\gamma}_{j+i-1} - \hat{\gamma}_{j-i}| - |\gamma_{j+i-1} - \gamma_{j-i}|) \ge h\epsilon\}}$$

$$\leq \Pr{\{\sum_{i=1}^{h} (|\hat{\gamma}_{j+i-1} - \hat{\gamma}_{j-i} - \gamma_{j+i-1} + \gamma_{j-i}|) \ge h\epsilon\}}$$

$$\leq \sum_{i=1}^{h} \Pr{\{|\hat{\gamma}_{j+i-1} - \gamma_{j+i-1} + \gamma_{j-i} - \hat{\gamma}_{j-i}| \ge \epsilon\}}$$

$$\leq \sum_{i=1}^{h} \Pr{\{(|\hat{\gamma}_{j+i-1} - \gamma_{j+i-1}| + |\gamma_{j-i} - \hat{\gamma}_{j-i}|) \ge \epsilon\}}$$

$$\leq \sum_{i=1}^{h} \left(\Pr{\{|\hat{\gamma}_{j+i-1} - \gamma_{j+i-1}| + |\gamma_{j-i} - \hat{\gamma}_{j-i}| \ge \frac{\epsilon}{2}\}} + \Pr{\{|\gamma_{j-i} - \hat{\gamma}_{j-i}| \ge \frac{\epsilon}{2}\}}\right)$$

$$\leq 2hc'_{1} \exp\left(-c_{2}n\epsilon^{2}\right),$$

where $c_2 = c_2'/4$. Same strategy is applied to the second term. Therefore, letting $c_1 = 4c_1'$, we have

$$\Pr\{|\hat{D}(j,h) - D(j,h)| \ge \epsilon\} \le hc_1 \exp(-c_2 n\epsilon^2). \tag{A.7}$$

A.2 Proofs of Theorems 2.1

The proof of Theorem 2.1 follows Theorem 1 in Wainwright (2009), by realizing that the error term in the transformed model is normally distributed and the spectral norm of the projection matrix is upper bounded by 1.

A.3 Proof of Theorem 2.2

We have stated that the swapped distribution is

$$[\mathbf{X}^*, \tilde{\mathbf{X}}]_{\text{swap}}^{\top}(\mathcal{G})\mathbf{y}^* \sim N([\mathbf{X}^*, \tilde{\mathbf{X}}]_{\text{swap}}^{\top}(\mathcal{G})\mathbf{X}^*\boldsymbol{\theta}_1, \sigma^2[\mathbf{X}^*, \tilde{\mathbf{X}}]_{\text{swap}}^{\top}(\mathcal{G})\mathbf{M}[\mathbf{X}^*, \tilde{\mathbf{X}}]_{\text{swap}}(\mathcal{G})). \tag{A.8}$$

Then the pairwise exchangeability would hold if only the mean and variance of swapped distribution (A.8) are invariant. As for the mean, the elements of $[\mathbf{X}^*, \tilde{\mathbf{X}}]_{\mathrm{swap}(\mathcal{G})}^{\top} \mathbf{X}^*$ are identical to $[\mathbf{X}^*, \tilde{\mathbf{X}}]^{\top} \mathbf{X}^*$ except for those computed from the jth column with $j \in \mathcal{G}$. Meanwhile, for $j \in \mathcal{G}$, we have $\theta_{1j} = 0$, as $\mathcal{G} \subset \mathcal{S}^c$. Therefore, $[\mathbf{X}^*, \tilde{\mathbf{X}}]_{\mathrm{swap}(\mathcal{G})}^{\top} \mathbf{X}^* \boldsymbol{\theta}_1 = [\mathbf{X}^*, \tilde{\mathbf{X}}]^{\top} \mathbf{X}^* \boldsymbol{\theta}_1$.

The variance in (A.8), on the other hand, can be rewritten as

$$\sigma^{2}[\mathbf{X}^{*}, \tilde{\mathbf{X}}]_{\text{swap}(\mathcal{G})}^{\top} \mathbf{M}[\mathbf{X}^{*}, \tilde{\mathbf{X}}]_{\text{swap}(\mathcal{G})} = \sigma^{2} \begin{pmatrix} \mathbf{X}_{\text{swap}(\mathcal{G})}^{*\top} \mathbf{M} \mathbf{X}_{\text{swap}(\mathcal{G})}^{*}, & \mathbf{X}_{\text{swap}(\mathcal{G})}^{*\top} \mathbf{M} \tilde{\mathbf{X}}_{\text{swap}(\mathcal{G})}^{*} \\ \tilde{\mathbf{X}}_{\text{swap}(\mathcal{G})}^{\top} \mathbf{M} \mathbf{X}_{\text{swap}(\mathcal{G})}^{*}, & \tilde{\mathbf{X}}_{\text{swap}(\mathcal{G})}^{\top} \mathbf{M} \tilde{\mathbf{X}}_{\text{swap}(\mathcal{G})}^{*} \end{pmatrix}, \quad (A.9)$$

where $\mathbf{Z}_{\text{swap}(\mathcal{G})}$, with slight abuse of the notation "swap(·)", represents substituting the the respective columns of matrix \mathbf{Z} in \mathcal{G} by their counterparts. Then the (i, j)th entry in the first block of (A.9) is indeed

$$\{\mathbf{X}_{\text{swap}}^{*\top}(\mathcal{G})\mathbf{M}\mathbf{X}_{\text{swap}}^{*}(\mathcal{G})\}_{(i,j)} = \begin{cases} X_{i}^{*\top}\mathbf{M}X_{j}^{*} = X_{i}^{*\top}X_{j}^{*} = \mathbf{\Sigma}_{(i,j)}^{*}, & \text{if } i \notin \mathcal{G}, \ j \notin \mathcal{G} \\ \tilde{X}_{i}^{\top}\mathbf{M}X_{j}^{*} = \tilde{X}_{i}^{\top}X_{j}^{*} = \mathbf{\Sigma}_{(i,j)}^{*}, & \text{if } i \in \mathcal{G}, \ j \notin \mathcal{G} \\ X_{i}^{*\top}\mathbf{M}\tilde{X}_{j} = X_{i}^{*\top}\tilde{X}_{j} = \mathbf{\Sigma}_{(i,j)}^{*}, & \text{if } i \notin \mathcal{G}, \ j \in \mathcal{G} \\ \tilde{X}_{i}^{\top}\mathbf{M}\tilde{X}_{j} = \{\mathbf{X}^{*\top}\mathbf{X}^{*}\}_{(i,j)} = \mathbf{\Sigma}_{(i,j)}^{*}, & \text{if } i \in \mathcal{G}, \ j \in \mathcal{G} \end{cases}$$

$$(A.10)$$

The equality of first three cases in (A.10) holds attributed to that $\mathbf{M}\mathbf{X}^* = \mathbf{M}^{\top}\mathbf{X}^* = \mathbf{X}^*$, and $\tilde{\mathbf{X}}$ is the GKnockoff of \mathbf{X}^* . Note that for the second and third cases, $i \neq j$ since they belong to different sets. For the last case in (A.10), Lemma A.1 in the appendix indicates that $\mathbf{M}\tilde{\mathbf{X}}$ is also a GKnockoff of \mathbf{X}^* , thus $\tilde{X}_i^{\top}\mathbf{M}\tilde{X}_j = \{(\mathbf{M}\tilde{\mathbf{X}})^{\top}\mathbf{M}\tilde{\mathbf{X}}\}_{(i,j)} = \{\mathbf{X}^{*\top}\mathbf{X}^*\}_{(i,j)} = \mathbf{\Sigma}_{(i,j)}^*$. In sum,

$$\mathbf{X}_{\text{swap}(\mathcal{G})}^{*\top} \mathbf{M} \mathbf{X}_{\text{swap}(\mathcal{G})}^{*} = \mathbf{\Sigma}^{*} = \mathbf{X}^{*\top} \mathbf{X}^{*} = \mathbf{X}^{*\top} \mathbf{M} \mathbf{X}^{*}. \tag{A.11}$$

Next, the (i, j)th entry in the second block of (A.9) is

$$\{\mathbf{X}_{\text{swap}}^{*\top}(\mathcal{G})\mathbf{M}\tilde{\mathbf{X}}_{\text{swap}}(\mathcal{G})\}_{(i,j)} = \begin{cases} X_{i}^{*\top}\mathbf{M}\tilde{X}_{j} = X_{i}^{*\top}\tilde{X}_{j}, & \text{if } i \notin \mathcal{G}, \ j \notin \mathcal{G} \\ \tilde{X}_{i}^{\top}\mathbf{M}\tilde{X}_{j} = \{\mathbf{X}^{*\top}\mathbf{X}^{*}\}_{(i,j)} = \boldsymbol{\Sigma}_{(i,j)}^{*}, & \text{if } i \in \mathcal{G}, \ j \notin \mathcal{G} \\ X_{i}^{*\top}\mathbf{M}X_{j}^{*} = X_{i}^{*\top}X_{j}^{*} = \boldsymbol{\Sigma}_{(i,j)}^{*}, & \text{if } i \notin \mathcal{G}, \ j \in \mathcal{G} \\ \tilde{X}_{i}^{\top}\mathbf{M}X_{j}^{*} = \tilde{X}_{i}^{\top}X_{j}^{*}, & \text{if } i \in \mathcal{G}, \ j \in \mathcal{G} \end{cases}$$

$$(A.12)$$

The second and third cases in (A.12) directly follow (A.10), where i and j are in distinct sets hence can not be equal. In the first and last cases, by the construction rule of GKnockoffs,

$$X_i^{*\top} \tilde{X}_j = \begin{cases} \boldsymbol{\Sigma}_{(i,j)}^* & \text{if } i \neq j \\ \boldsymbol{\Sigma}_{(i,i)}^* - s_i & \text{if } i = j \end{cases}$$
 (A.13)

Therefore,

$$\{\mathbf{X}_{\text{swap}(\mathcal{G})}^{*\top}\mathbf{M}\tilde{\mathbf{X}}_{\text{swap}(\mathcal{G})}\} = \mathbf{\Sigma}^{*} - \text{diag}(\mathbf{s}) = \mathbf{X}^{*\top}\mathbf{M}\tilde{\mathbf{X}}.$$
(A.14)

Similar arguments applying to the remaining two blocks of (A.9), we easily obtain

$$[\mathbf{X}^*, \tilde{\mathbf{X}}]_{\text{swap}}^{\top}(\mathcal{G}) \mathbf{M} [\mathbf{X}^*, \tilde{\mathbf{X}}]_{\text{swap}}(\mathcal{G}) = \begin{pmatrix} \mathbf{\Sigma}^*, & \mathbf{\Sigma}^* - \text{diag}(\mathbf{s}) \\ \mathbf{\Sigma}^* - \text{diag}(\mathbf{s}), & \mathbf{\Sigma}^* \end{pmatrix} = [\mathbf{X}^*, \tilde{\mathbf{X}}]^{\top} \mathbf{M} [\mathbf{X}^* \tilde{\mathbf{X}}]. \quad (A.15)$$

The pairwise exchangeability subsequently holds.

A.4 Proof of Theorem 2.3

In light of Lemma 2.1, we can apply Lemma 1 in Barber and Candès (2015) to prove the theorem.

A.5 Proof of Theorem 2.4

Denote the GKnockoff of $\begin{bmatrix} \mathbf{X}^* \\ \mathbf{0} \end{bmatrix}$ as $\begin{bmatrix} \tilde{\mathbf{X}}_1 \\ \tilde{\mathbf{X}}_2 \end{bmatrix}$, then by the construction of knockoffs, we have,

$$\mathbf{X}^{*\top}\mathbf{X}^{*} = \begin{bmatrix} \mathbf{X}^{*\top}, \mathbf{0}^{\top} \end{bmatrix} \begin{bmatrix} \mathbf{X}^{*} \\ \mathbf{0} \end{bmatrix} = \begin{bmatrix} \tilde{\mathbf{X}}_{1}^{\top}, \tilde{\mathbf{X}}_{2}^{\top} \end{bmatrix} \begin{bmatrix} \tilde{\mathbf{X}}_{1} \\ \tilde{\mathbf{X}}_{2} \end{bmatrix} \triangleq \mathbf{\Sigma}_{a}^{*}$$
(A.16)

and

$$\begin{bmatrix} \mathbf{X}^{*\top}, \mathbf{0}^{\top} \end{bmatrix} \begin{bmatrix} \tilde{\mathbf{X}}_1 \\ \tilde{\mathbf{X}}_2 \end{bmatrix} = \mathbf{X}^{*\top} \tilde{\mathbf{X}}_1 = \mathbf{\Sigma}_a^* - \operatorname{diag}(\mathbf{s})$$
(A.17)

The distribution of $\begin{bmatrix} \mathbf{X}^{*\top}, & \mathbf{0}^{\top} \\ \tilde{\mathbf{X}}_{1}^{\top}, & \tilde{\mathbf{X}}_{2}^{\top} \end{bmatrix} \begin{bmatrix} \mathbf{y}^{*} \\ \mathbf{y}_{a}^{*} \end{bmatrix}$ is

$$\begin{bmatrix} \mathbf{X}^{*\top}, & \mathbf{0}^{\top} \\ \tilde{\mathbf{X}}_{1}^{\top}, & \tilde{\mathbf{X}}_{2}^{\top} \end{bmatrix} \begin{bmatrix} \mathbf{y}^{*} \\ \mathbf{y}_{a}^{*} \end{bmatrix} \sim N \begin{pmatrix} \begin{bmatrix} \mathbf{X}^{*\top}, & \mathbf{0}^{\top} \\ \tilde{\mathbf{X}}_{1}^{\top}, & \tilde{\mathbf{X}}_{2}^{\top} \end{bmatrix} \begin{bmatrix} \mathbf{X}^{*} \\ \mathbf{0} \end{bmatrix} \cdot \boldsymbol{\theta}_{1}, \sigma^{2} \mathbf{A} \end{pmatrix}$$
(A.18)

where

$$\mathbf{A} = \begin{bmatrix} \mathbf{X}^{*\top}, & \mathbf{0}^{\top} \\ \tilde{\mathbf{X}}_{1}^{\top}, & \tilde{\mathbf{X}}_{2}^{\top} \end{bmatrix} \begin{bmatrix} \mathbf{M}, & \mathbf{0} \\ \mathbf{0}, & \mathbf{I} \end{bmatrix} \begin{bmatrix} \mathbf{X}^{*}, & \tilde{\mathbf{X}}_{1} \\ \mathbf{0}, & \tilde{\mathbf{X}}_{2} \end{bmatrix}$$
(A.19)

and the distribution of $\begin{bmatrix} \mathbf{X}_{\mathrm{swap}\,(\mathcal{G})}^{*\top}, & \mathbf{0}_{\mathrm{swap}\,(\mathcal{G})}^{\top} \\ \tilde{\mathbf{X}}_{1,\mathrm{swap}\,(\mathcal{G})}^{\top}, & \tilde{\mathbf{X}}_{2,\mathrm{swap}\,(\mathcal{G})}^{\top} \end{bmatrix} \begin{bmatrix} \mathbf{y}^* \\ \mathbf{y}_a^* \end{bmatrix} \text{ is }$

$$\begin{bmatrix} \mathbf{X}_{\mathrm{swap}\,(\mathcal{G})}^{*\top}, & \mathbf{0}_{\mathrm{swap}\,(\mathcal{G})}^{\top} \\ \tilde{\mathbf{X}}_{1,\mathrm{swap}\,(\mathcal{G})}^{\top}, & \tilde{\mathbf{X}}_{2,\mathrm{swap}\,(\mathcal{G})}^{\top} \end{bmatrix} \begin{bmatrix} \mathbf{y}^{*} \\ \mathbf{y}_{a}^{*} \end{bmatrix} \sim N \begin{pmatrix} \begin{bmatrix} \mathbf{X}_{\mathrm{swap}\,(\mathcal{G})}^{*\top}, & \mathbf{0}_{\mathrm{swap}\,(\mathcal{G})}^{\top} \\ \tilde{\mathbf{X}}_{1,\mathrm{swap}\,(\mathcal{G})}^{\top}, & \tilde{\mathbf{X}}_{2,\mathrm{swap}\,(\mathcal{G})}^{\top} \end{bmatrix} \begin{bmatrix} \mathbf{X}^{*} \\ \mathbf{0} \end{bmatrix} \cdot \boldsymbol{\theta}_{1}, \sigma^{2} \mathbf{A}_{\mathrm{swap}\,(\mathcal{G})} \end{pmatrix}$$
(A.20)

where $\mathbf{A}_{\mathrm{swap}\,(\mathcal{G})}$ is

$$\mathbf{A}_{\text{swap}}(\mathcal{G}) = \begin{bmatrix} \mathbf{X}_{\text{swap}}^{*\top}(\mathcal{G}), & \mathbf{0}_{\text{swap}}^{\top}(\mathcal{G}) \\ \tilde{\mathbf{X}}_{1,\text{swap}}^{\top}(\mathcal{G}), & \tilde{\mathbf{X}}_{2,\text{swap}}^{\top}(\mathcal{G}) \end{bmatrix} \begin{bmatrix} \mathbf{M}, & \mathbf{0} \\ \mathbf{0}, & \mathbf{I} \end{bmatrix} \begin{bmatrix} \mathbf{X}_{\text{swap}}^{*}(\mathcal{G}), & \tilde{\mathbf{X}}_{1,\text{swap}}(\mathcal{G}) \\ \mathbf{0}_{\text{swap}}(\mathcal{G}), & \tilde{\mathbf{X}}_{2,\text{swap}}(\mathcal{G}) \end{bmatrix}$$
(A.21)

It is trivial that the mean of distribution remains after swapping is the same if $j \in \mathcal{S}^c$ by using the value fact of $\theta_{1,j} = 0$ for $j \in \mathcal{S}$. Next, we need to show $\mathbf{A} = \mathbf{A}_{\text{swap}(\mathcal{G})}$. Define

$$\mathbf{M}^{\dagger} = \begin{bmatrix} \mathbf{M}, & \mathbf{0} \\ \mathbf{0}, & \mathbf{I} \end{bmatrix}. \tag{A.22}$$

One can see that \mathbf{M}^{\dagger} is symmetric and,

$$\mathbf{M}^{\dagger} \begin{bmatrix} \mathbf{X}^* \\ \mathbf{0} \end{bmatrix} = \begin{bmatrix} \mathbf{M}\mathbf{X}^* \\ \mathbf{0} \end{bmatrix} = \begin{bmatrix} \mathbf{X}^* \\ \mathbf{0} \end{bmatrix}$$
 (A.23)

then by Lemma A.1, $\tilde{\mathbf{X}}_a = \mathbf{M}^{\dagger} \begin{bmatrix} \tilde{\mathbf{X}}_1 \\ \tilde{\mathbf{X}}_2 \end{bmatrix}$ is also a GKnockoff of $\begin{bmatrix} \mathbf{X}^* \\ \mathbf{0} \end{bmatrix}$. Using this fact, we can simplified \mathbf{A} as

$$\mathbf{A} = \begin{bmatrix} \mathbf{X}^{*\top}, & \mathbf{0}^{\top} \\ \tilde{\mathbf{X}}_{1}^{\top}, & \tilde{\mathbf{X}}_{2}^{\top} \end{bmatrix} \begin{bmatrix} \mathbf{M}, & \mathbf{0} \\ \mathbf{0}, & \mathbf{I} \end{bmatrix} \begin{bmatrix} \mathbf{X}^{*}, & \tilde{\mathbf{X}}_{1} \\ \mathbf{0}, & \tilde{\mathbf{X}}_{2} \end{bmatrix}$$

$$= \begin{bmatrix} \mathbf{X}^{*\top}\mathbf{M}\mathbf{X}^{*}, & \mathbf{X}^{*\top}\mathbf{M}\tilde{\mathbf{X}}_{1} \\ \tilde{\mathbf{X}}_{1}^{\top}\mathbf{M}\mathbf{X}^{*}, & \tilde{\mathbf{X}}_{1}^{\top}\mathbf{M}\tilde{\mathbf{X}}_{1} + \tilde{\mathbf{X}}_{2}^{\top}\tilde{\mathbf{X}}_{2} \end{bmatrix}.$$
(A.24)

By the construction of GKnockoff, we have shown that $\mathbf{X}^{*\top}\mathbf{M}\mathbf{X}^{*} = \mathbf{X}^{*\top}\mathbf{X}^{*} = \mathbf{\Sigma}_{a}^{*}, \ \mathbf{X}^{*\top}\mathbf{M}\tilde{\mathbf{X}}_{1} = \mathbf{X}^{*\top}\mathbf{X}^{*}\mathbf{X}^{*\top}\mathbf{X}^{*}\mathbf{X}^{*\top}\mathbf{X}^{*}\mathbf{X}^{*\top}\mathbf{X}^{*}\mathbf{X}^{*}\mathbf{X}^{*\top}\mathbf{X}^{*}\mathbf{X}^{*\top}\mathbf{X}^{*\top}\mathbf{X}^{*\top}\mathbf{X}^{*\top}\mathbf{X}^{*\top}\mathbf{X}^{*\top}\mathbf{X}^{*\top}\mathbf{X}^{*\top}\mathbf{X}^{*\top}\mathbf{X}^{*\top}\mathbf{X}^{*\top}\mathbf{X}^{*\top}\mathbf{X}^{*\top}\mathbf{X}^{*\top}\mathbf{$

$$\mathbf{X}^{*\top}\tilde{\mathbf{X}}_{1} = \mathbf{\Sigma}_{a}^{*} - \operatorname{diag}(\mathbf{s}) \text{ and } \tilde{\mathbf{X}}_{1}^{\top}\mathbf{M}\tilde{\mathbf{X}}_{1} + \tilde{\mathbf{X}}_{2}^{\top}\tilde{\mathbf{X}}_{2} = \begin{bmatrix} \tilde{\mathbf{X}}_{1}^{\top}, \tilde{\mathbf{X}}_{2}^{\top} \end{bmatrix} \begin{bmatrix} \mathbf{M}, & \mathbf{0} \\ \mathbf{0}, & \mathbf{I} \end{bmatrix}^{2} \begin{bmatrix} \tilde{\mathbf{X}}_{1} \\ \tilde{\mathbf{X}}_{2} \end{bmatrix} = \tilde{\mathbf{X}}_{a}^{\top}\tilde{\mathbf{X}}_{a} = \mathbf{\Sigma}_{a}^{*},$$
therefore

$$\mathbf{A} = \begin{bmatrix} \mathbf{\Sigma}_a^*, & \mathbf{\Sigma}_a^* - \operatorname{diag}(\mathbf{s}) \\ \mathbf{\Sigma}_a^* - \operatorname{diag}(\mathbf{s}), & \mathbf{\Sigma}_a^* \end{bmatrix}. \tag{A.25}$$

Then we need to show $\mathbf{A}_{\text{swap}(\mathcal{G})} = \mathbf{A}$, where

$$\begin{split} \mathbf{A}_{\mathrm{swap}\,(\mathcal{G})} &= \begin{bmatrix} \mathbf{X}_{\mathrm{swap}\,(\mathcal{G})}^{\top}, & \mathbf{0}_{\mathrm{swap}\,(\mathcal{G})}^{\top} \\ \tilde{\mathbf{X}}_{1,\mathrm{swap}\,(\mathcal{G})}^{\top}, & \tilde{\mathbf{X}}_{2,\mathrm{swap}\,(\mathcal{G})}^{\top} \end{bmatrix} \begin{bmatrix} \mathbf{M}, & \mathbf{0} \\ \mathbf{0}, & \mathbf{I} \end{bmatrix} \begin{bmatrix} \mathbf{X}_{\mathrm{swap}\,(\mathcal{G})}^{*}, & \tilde{\mathbf{X}}_{1,\mathrm{swap}\,(\mathcal{G})}^{*} \end{bmatrix} \\ \mathbf{0}_{\mathrm{swap}\,(\mathcal{G})}, & \tilde{\mathbf{X}}_{2,\mathrm{swap}\,(\mathcal{G})}^{*} \end{bmatrix} \\ &= \begin{bmatrix} \mathbf{X}_{\mathrm{swap}\,(\mathcal{G})}^{*\top} \mathbf{M} \mathbf{X}_{\mathrm{swap}\,(\mathcal{G})}^{*} + \mathbf{0}_{\mathrm{swap}\,(\mathcal{G})}^{\top} \mathbf{0}_{\mathrm{swap}\,(\mathcal{G})}, & \mathbf{X}_{\mathrm{swap}\,(\mathcal{G})}^{*\top} \mathbf{M} \tilde{\mathbf{X}}_{1,\mathrm{swap}\,(\mathcal{G})} + \mathbf{0}_{\mathrm{swap}\,(\mathcal{G})}^{\top} \tilde{\mathbf{X}}_{2,\mathrm{swap}\,(\mathcal{G})} \\ \tilde{\mathbf{X}}_{1,\mathrm{swap}\,(\mathcal{G})}^{\top} \mathbf{M} \mathbf{X}_{\mathrm{swap}\,(\mathcal{G})}^{*} + \tilde{\mathbf{X}}_{2,\mathrm{swap}\,(\mathcal{G})}^{\top} \mathbf{0}_{\mathrm{swap}\,(\mathcal{G})}, & \tilde{\mathbf{X}}_{1,\mathrm{swap}\,(\mathcal{G})}^{\top} \mathbf{M} \tilde{\mathbf{X}}_{1,\mathrm{swap}\,(\mathcal{G})}^{*} + \mathbf{0}_{\mathrm{swap}\,(\mathcal{G})}^{\top} \tilde{\mathbf{X}}_{2,\mathrm{swap}\,(\mathcal{G})} \end{bmatrix}. \end{split}$$

For the first block of $\mathbf{A}_{\text{swap}(\mathcal{G})}$, we see that

$$\mathbf{X}_{\text{swap}}^{*\top}(\mathcal{G})\mathbf{M}\mathbf{X}_{\text{swap}}^{*}(\mathcal{G}) + \mathbf{0}_{\text{swap}}^{\top}(\mathcal{G})\mathbf{0}_{\text{swap}}(\mathcal{G}) = \begin{cases} X_{i}^{*\top}\mathbf{M}X_{j}^{*}, & i \notin \mathcal{G}, j \notin \mathcal{G} \\ \tilde{X}_{1,i}^{\top}\mathbf{M}X_{j}^{*}, & i \in \mathcal{G}, j \notin \mathcal{G} \\ X_{i}^{*\top}\mathbf{M}\tilde{X}_{1,j}, & i \notin \mathcal{G}, j \in \mathcal{G} \end{cases}$$

$$\tilde{X}_{1,i}^{\top}\mathbf{M}\tilde{X}_{1,j} + \tilde{X}_{2,i}^{\top}\tilde{X}_{2,j}, & i \in \mathcal{G}, i \in \mathcal{G} \end{cases}$$
(A.27)

Since $\mathbf{M}\mathbf{X}^* = \mathbf{X}^*$, we have $X_i^{*\top}\mathbf{M}X_j^* = X_i^{*\top}X_j^* = \boldsymbol{\Sigma}_{a(i,j)}^*$, by the construction of \tilde{X}_1 and $i \neq j$, we further conclude that $\tilde{X}_{1,i}^{\top}\mathbf{M}X_j^* = \tilde{X}_{1,i}^{\top}X_j^* = \boldsymbol{\Sigma}_{a(i,j)}^*$. Recall $\mathbf{M}\begin{bmatrix} \tilde{\mathbf{X}}_1 \\ \tilde{\mathbf{X}}_2 \end{bmatrix}$ is the knockoff of $\begin{bmatrix} \mathbf{X}^* \\ \mathbf{0} \end{bmatrix}$, therefore $\tilde{X}_{1,i}^{\top}\mathbf{M}\tilde{X}_{1,j} + \tilde{X}_{2,i}^{\top}\tilde{X}_{2,j} = \boldsymbol{\Sigma}_{a(i,j)}^*$. Sum it up, the first block of $\mathbf{A}_{\mathrm{swap}(\mathcal{G})}$ equals to $\boldsymbol{\Sigma}_a^*$. Using the same idea, we can show the $\mathbf{X}_{\mathrm{swap}(\mathcal{G})}^{*\top}\mathbf{M}\tilde{\mathbf{Z}}_{1,\mathrm{swap}(\mathcal{G})} + \mathbf{0}_{\mathrm{swap}(\mathcal{G})}^{\top}\tilde{\mathbf{X}}_{2,\mathrm{swap}(\mathcal{G})} = \tilde{\mathbf{X}}_{1,\mathrm{swap}(\mathcal{G})}^{\top}\mathbf{M}\mathbf{X}_{\mathrm{swap}(\mathcal{G})}^* + \tilde{\mathbf{X}}_{2,\mathrm{swap}(\mathcal{G})}^{\top}\tilde{\mathbf{X}}_{2,\mathrm{swap}(\mathcal{G})} = \tilde{\mathbf{X}}_{1,\mathrm{swap}(\mathcal{G})}^{\top}\mathbf{M}\mathbf{X}_{\mathrm{swap}(\mathcal{G})}^* + \tilde{\mathbf{X}}_{2,\mathrm{swap}(\mathcal{G})}^{\top}\tilde{\mathbf{X}}_{2,\mathrm{swap}(\mathcal{G})}^{\top}\tilde{\mathbf{X}}_{2,\mathrm{swap}(\mathcal{G})} = \boldsymbol{\Sigma}_a^*$. As a result, we have $\mathbf{A}_{\mathrm{swap}(\mathcal{G})} = \mathbf{A}$. Then we obtain the pairwise exchangeability,

$$\begin{bmatrix} \mathbf{X}^{*\top}, & \mathbf{0}^{\top} \\ \tilde{\mathbf{X}}_{1}^{\top}, & \tilde{\mathbf{X}}_{2}^{\top} \end{bmatrix} \begin{bmatrix} \mathbf{y}^{*} \\ \mathbf{y}_{a}^{*} \end{bmatrix} \stackrel{d}{=} \begin{bmatrix} \mathbf{X}_{\text{swap}}^{*\top}(\mathcal{G}), & \mathbf{0}_{\text{swap}}^{\top}(\mathcal{G}) \\ \tilde{\mathbf{X}}_{1,\text{swap}}^{\top}(\mathcal{G}), & \tilde{\mathbf{X}}_{2,\text{swap}}^{\top}(\mathcal{G}) \end{bmatrix} \begin{bmatrix} \mathbf{y}^{*} \\ \mathbf{y}_{a}^{*} \end{bmatrix}.$$
(A.28)

By the antisymmetry and sufficiency of w, Theorem 2.4 naturally follows.

A.6 Proof of Theorem 3.1

Recall that the Lemma A.3 states a exponential-type deviation inequality for the screening criteria $\hat{\mathbf{D}}(j,h)$

$$\Pr\{|\hat{\mathbf{D}}(j,h) - \mathbf{D}(j,h)| \ge \epsilon\} \le hc_1 \exp(-c_2 n\epsilon^2). \tag{A.29}$$

where c_1 and c_2 are some positive constants. We consider the complement $\mathcal{S} \nsubseteq \hat{\mathcal{A}}(\vartheta)$, meaning that there is at least one $k \in \mathcal{S}$ such that $k \in \hat{\mathcal{A}}(\vartheta)$, for the choice of $\vartheta > 0$ in Theorem 3.1, we have

$$\Pr\left(\mathcal{S} \nsubseteq \hat{\mathcal{A}}(\vartheta)\right) = \Pr\left(\bigcup_{j \in \mathcal{S}} \{j \notin \hat{\mathcal{A}}(\vartheta)\}\right) \le \sum_{j \in \mathcal{S}} \Pr\left(\hat{\mathbf{D}}(j, h) \le \vartheta\right),\tag{A.30}$$

Condition 3.1 implies the population screening criteria for any $j \in \mathcal{S}$ has $D(j,h) \geq 2c_3n^{-\kappa}$, in company with the choice of $\vartheta \leq \min_{j \in \mathcal{S}} D(j,h)/2 \leq c_3n^{-\kappa}$, we have $D(j,h) \geq c_3n^{-\kappa} + \vartheta$. As a result, the event $\hat{D}(j,h) \leq \vartheta$ implies

$$D(j,h) - \hat{D}(j,h) \ge c_3 n^{-\kappa} \tag{A.31}$$

then the probability of complement event

$$\Pr\left(\mathcal{S} \nsubseteq \hat{\mathcal{A}}(\vartheta)\right) \leq \sum_{j \in \mathcal{S}} \Pr\left(\mathcal{D}(j,h) - \hat{\mathcal{D}}(j,h) \geq c_3 n^{-\kappa}\right)$$

$$\leq \sum_{j \in \mathcal{S}} \Pr\left(|\mathcal{D}(j,h) - \hat{\mathcal{D}}(j,h)| \geq c_3 n^{-\kappa}\right)$$

$$\leq shc_1 \exp(-c_2 c_3^2 n^{1-2\kappa}) = shc_1 \exp(-c_4 n^{1-2\kappa})$$
(A.32)

where $c_4 = c_2 c_3^2$, thus $\Pr\left(S \subseteq \hat{\mathcal{A}}(\vartheta)\right) \ge 1 - O(sh \exp(-c_4 n^{1-2\kappa}))$.

A.7 Proof of Theorem 3.2

Theorem 3.2 trivially holds on the basis of Theorem 2.3 and 3.1.

References

Avanesov, V. and N. Buzun (2018). Change-point detection in high-dimensional covariance structure. *Electronic Journal of Statistics* 12(2), 3254–3294.

Barber, R. F. and E. Candès (2015). Controlling the false discovery rate via knockoffs. *The Annals of Statistics* 43(5), 2055–2085.

Barber, R. F. and E. Candès (2019). A knockoff filter for high-dimensional selective inference.

Annals of Statistics 47(5), 2504–2537.

Benjamini, Y. (2010). Discovering the false discovery rate. Journal of the Royal Statistical Society: Series B (Statistical Methodology) 72(4), 405–416.

Benjamini, Y. and Y. Hochberg (1995). Controlling the false discovery rate: a practical and powerful

- approach to multiple testing. Journal of the Royal Statistical Society: Series B (Statistical Methodology) 57(1), 289–300.
- Benjamini, Y. and D. Yekutieli (2001). The control of the false discovery rate in multiple testing under dependency. *The Annals of Statistics* 29(4), 1165–1188.
- Candès, E., Y. Fan, L. Janson, and J. Lv (2018). Panning for gold: 'model-X' knockoffs for high dimensional controlled variable selection. *Journal of the Royal Statistical Society: Series B* (Statistical Methodology) 80(3), 551–577.
- Chen, H. and N. Zhang (2015). Graph-based change-point detection. *The Annals of Statistics* 43(1), 139–176.
- Cho, H. and P. Fryzlewicz (2015). Multiple-change-point detection for high dimensional time series via sparsified binary segmentation. *Journal of the Royal Statistical Society: Series B: (Statistical Methodology)* 77(2), 475–507.
- Dai, R. and R. F. Barber (2016). The knockoff filter for FDR control in group-sparse and multitask regression. *Proceedings of The 33rd International Conference on Machine Learning*, 1851–1859.
- Dette, H., G. Pan, and Q. Yang (2020). Estimating a change point in a sequence of very highdimensional covariance matrices. *Journal of the American Statistical Association*, forthcoming.
- Fan, J., S. Guo, and N. Hao (2012). Variance estimation using refitted cross-validation in ultrahigh dimensional regression. Journal of the Royal Statistical Society: Series B (Statistical Methodology) 74(1), 37–65.
- Fan, J., Y. Ke, and K. Wang (2020). Factor-adjusted regularized model selection. *Journal of Econometrics* 216(1), 71–85.
- Fan, J. and R. Li (2001). Variable selection via nonconcave penalized likelihood and its oracle properties. *Journal of the American Statistical Association* 96 (456), 1348–1360.
- Fan, J., R. Li, C.-H. Zhang, and H. Zou (2020). Statistical Foundations of Data Science. Chapman and Hall/CRC.

- Fan, J. and J. Lv (2008). Sure independent screening for ultrahigh dimensional feature space.

 Journal of the Royal Statistical Society: Series B (Statistical Methodology) 70(5), 849–911.
- Fan, J. and J. Lv (2018). Sure independence screening. Wiley StatsRef: Statistics Reference Online, 1–8.
- Fan, Y., E. Demirkaya, G. Li, and J. Lv (2018). RANK: large-scale inference with graphical nonlinear knockoffs. *Journal of the American Statistical Association* 115(529), 362–379.
- Fan, Y., J. Lv, M. Sharifvaghefi, and Y. Uematsu (2020). IPAD: stable interpretable forecasting with knockoffs inference. *Journal of the American Statistical Association* 115 (532), 1822–1834.
- G'Sell, M. G., S. Wager, A. Chouldechova, and R. Tibshirani (2016). Sequential selection procedures and false discovery rate control. *Journal of the Royal Statistical Society. Series B (Statistical Methodology)* 78(2), 423–444.
- Harchaoui, Z. and C. Lévy-Leduc (2007). Catching change-points with lasso. Advances in Neural Information Processing Systems (NIPS 2007).
- Hsiao, C., Y. Xie, and Q. Zhou (2021). Factor dimension determination for panel interactive effects models: an orthogonal projection approach. *Computational Statistics* 36(2), 1481–1497.
- Jiang, F., Z. Zhao, and X. Shao (2020). Time series analysis of COVID-19 infection curve: A change-point perspective. *Journal of Econometrics*, forthcoming.
- Ke, Z. T., J. Fan, and Y. Wu (2015). Homogeneity pursuit. Journal of the American Statistical Association 110(509), 175–194.
- Ke, Z. T., J. Jin, and J. Fan (2014). Covariate assisted screening and estimation. *The Annals of Statistics* 42(2), 2202–2242.
- Li, C. and R. Li (2021). Linear hypothesis testing in linear models with high-dimensional responses.

 Journal of the American Statistical Association, forthcoming.
- Li, R., W. Zhong, and L. Zhu (2012). Feature screening via distance correlation learning. *Journal* of the American Statistical Association 107(499), 1129–1139.

- Liu, J., R. Li, and R. Wu (2014). Feature selection for varying coefficient models with ultrahigh-dimensional covariates. *Journal of the American Statistical Association* 109(505), 266–274.
- Liu, J., W. Zhong, and R. Li (2015). A selective overview of feature screening for ultrahighdimensional data. *Science China Mathematics* 58(10), 1–22.
- Liu, W., Y. Ke, J. Liu, and R. Li (2021). Model-free feature screening and FDR control with knockoff features. *Journal of the American Statistical Association*, forthcoming.
- Lu, Y. Y., Y. Fan, J. Lv, and W. S. Noble (2018). DeepPINK: reproducible feature selection in deep neural networks. *Advances in Neural Information Processing Systems (NIPS 2018)*.
- Ma, S., R. Li, and C.-L. Tsai (2017). Variable screening via quantile partial correlation. *Journal* of the American Statistical Association 112(518), 650–663.
- Mai, Q. and H. Zou (2015). The fused Kolmogorov filter: A nonparametric model-free screening method. The Annals of Statistics 43(4), 1471–1497.
- Niu, Y. S., N. Hao, and H. Zhang (2016). Multiple change-point detection: A selective overview. Statistical Science 31(4), 611–623.
- Niu, Y. S. and H. Zhang (2012). The screening and ranking algorithm to detect DNA copy number variations. The Annals of Applied Statistics 6(3), 1306–1326.
- Ramey, V. A. (2016). Macroeconomic shocks and their propagation. *Handbook of Macroeconomics* 2, 71–162.
- Rojas, C. R. and B. Wahlberg (2014). On change point detection using the fused lasso method. arXiv preprint arXiv:1401.5408.
- Romano, Y., M. Sesia, and E. Candès (2020). Deep knockoffs. *Journal of the American Statistical Association* 115(532), 1861–1872.
- Su, W., M. Bogdan, and E. Candès (2017). False discoveries occur early on the lasso path. *Annals of Statistics* 45(5), 2133–2150.

- Tang, L. and P. X. Song (2016). Fused lasso approach in regression coefficients clustering-learning parameter heterogeneity in data integration. *Journal of Machine Learning Research* 17(113), 1–23.
- Tibshirani, R. (1996). Regression shrinkage and selection via the lasso. *Journal of the Royal Statistical Society: Series B (Statistical Methodology)* 51(1), 267–288.
- Tibshirani, R., M. Saunders, S. Rosset, J. Zhu, and K. Knight (2005). Sparsity and smoothness via the fused lasso. *Journal of the Royal Statistical Society: Series B (Statistical Methodology)* 67(1), 91–108.
- Tibshirani, R. J. and J. Taylor (2011). The solution path of the generalized lasso. *The Annals of Statistics* 39(3), 1335–1371.
- Wainwright, M. J. (2009). Sharp thresholds for high-dimensional and noisy sparsity recovery using l_1 -constrained quadratic programming. *IEEE Transactions on Information Theory* 55(5), 2183–2202.
- Wang, D., Y. Yu, and A. Rinaldo (2020). Optimal covariance change point detection in high dimension. *Bernoulli*, forthcoming.
- Wang, F., L. Wang, and P. X.-K. Song (2016). Fused lasso with the adaptation of parameter ordering in combining multiple studies with repeated measurements. *Biometrics* 72(4), 1184–1193.
- Wang, G., C. Zou, and G. Yin (2018). Change-point detection in multinomial data with a large number of categories. *The Annals of Statistics* 46(5), 2020 2044.
- Wasserman, L. and K. Roeder (2009). High dimensional variable selection. *Annals of Statistics* 37(5A), 2178–2201.
- Weinstein, A., R. Barber, and E. Candès (2017). A power and prediction analysis for knockoffs with lasso statistics. arXiv preprint arXiv:1712.06465.
- Xiao, D., Y. Ke, and R. Li (2021). Homogeneity structure learning in large-scale panel data with heavy-tailed errors. *Journal of Machine Learning Research* 22(13), 1–42.

- Zhang, C.-H. (2010). Nearly unbiased variable selection under minimax concave penalty. The Annals of Statistics 38(2), 894 942.
- Zhao, P. and B. Yu (2006). On model selection consistency of lasso. The Journal of Machine Learning Research 7(90), 2541–2563.
- Zou, C., G. Yin, L. Feng, and Z. Wang (2014). Nonparametric maximum likelihood approach to multiple change-point problems. *The Annals of Statistics* 42(3), 970–1002.
- Zou, H. and R. Li (2008). One-step sparse estimates in nonconcave penalized likelihood models.

 The Annals of Statistics 36(4), 1509 1533.